Fabrication, Characterization and Testing of Copper based Reinforced with $GO/MoS_2/Ti_3SiC_2$ MAX Phase

Ruth Samson Tsege

A Thesis Submitted to Department of Mechanical Engineering

School of Mechanical, Chemical and Materials Engineering

Presented in Partial Fulfillment of the Requirement for the Degree of

Master's in Manufacturing Engineering

Office of Graduate Studies

Adama Science and Technology University

May - 2024

Adama, Ethiopia

Fabrication, Characterization and Testing of Copper based Reinforced with GO/MoS_2/Ti_3SiC_2 MAX Phase

Ruth Samson Tsege

Advisor: Dr. Devendra Kumar Sinha

A Thesis Submitted to Department of Mechanical Engineering School of Mechanical, Chemical and Materials Engineering

Presented in Partial Fulfillment of the Requirement for the Degree of Master's in Manufacturing Engineering

Office of Graduate Studies
Adama Science and Technology University

May - 2024
Adama, Ethiopia

DECLARATION

I hereby declare that this Master Thesis entitled "**Fabrication, Characterization and Testing of Copper based Reinforced with GO/MoS_2/Ti_3SiC_2 MAX Phase**" is my original work. That is, it has not been submitted for the award of any academic degree, diploma or certificate in any other university. All sources of materials that are used for this thesis have been duly acknowledged through citation.

Ruth Samson Tsege		27/06/2024
Name	Signature	Date

RECOMMENDATION

We, the advisors of this thesis, hereby certify that we have read the final version of the thesis entitled "**Fabrication, Characterization and Testing of Copper based Reinforced with GO/MoS_2/Ti_3SiC_2 MAX Phase**" Prepared under our guidance by Ruth Samson Tsege submitted in partial fulfillment of the requirements for the degree of Mater's of Science in Manufacturing Engineering. Therefore, we recommend the submission of the final revised version of the thesis to the department following the applicable procedures.

Dr. Devendra Kumar Sinha		28/06/2024
Advisor	Signature	Date
Co-advisor	Signature	Date

APPROVAL SHEET

I, the advisors of the thesis entitled "**Fabrication, Characterization and Testing of Copper based Reinforced with GO/MoS_2/Ti_3SiC_2 MAX Phase**" and developed by **Ruth Samson Tsege**, hereby certify that the recommendation and suggestions made by the board of examiners are appropriately incorporated into the final version of the thesis.

Dr. Devendra Kumar Sinha		28/06/2024
Major Advisor/Supervisor	Signature	Date

We, the undersigned, members of the Board of Examiners of the thesis by **Ruth Samson Tsege** have read and evaluated the thesis entitled "**Fabrication, Characterization and Testing of Copper based Reinforced with GO/MoS_2/Ti_3SiC_2 MAX Phase**" and examined the candidate during open defense. This is, therefore, to certify that the thesis is accepted for partial fulfillment of the requirement of the degree of Master of Science in **Manufacturing Engineering.**

Chairperson	Signature	Date
Internal Examiner	Signature	Date
Dr.Mesfin Gizaw		June 27/2024
Eternal Examiner	Signature	Date

Finally, approval and acceptance of the thesis is contingent upon the submission of its final copy to the Office of Postgraduate Studies (OPGS) through the Department Graduate Council (DGC) and School Graduate Committee (SGC).

Department Head	Signature	Date
School Dean	Signature	Date
Office of Postgraduate Studies, Dean	Signature	Date

ACKNOWLEDGEMENT

I would like to express my sincere gratitude to my advisors, Dr. Devendra Kumar Sinha and Dr. Getinet Asrat Mengesha, for their continuous support and guidance throughout this process. Additionally, I want to thank Mr. Dagmawi Hailu (Ph.D. candidate) for always being available to provide me with valuable advice whenever I needed it the most.

Furthermore, I would like to extend my heartfelt thanks to the departments of Mechanical Engineering, Material Science and Engineering, and Applied Chemistry at ASTU, as well as the Mechanical Engineering department at AASTU, for granting me access to various resources, facilities, and equipment for conducting machining, testing, and characterization.

Lastly, I would like to express my deep appreciation to all the individuals who have assisted me in any way during the preparation of this paperwork. Your contribution deserves great respect. Thank you all!

Table of Contents

LIST OF TABLES

LIST OF FIGURES

LIST OF ACRONYMS AND ABBREVIATION

ASTM	American society for testing and materials
Cu15000	Copper Zirconium
Cu-MMC	copper metal matrix
FTIR	FOURIER Transform Infrared Spectroscopy
GO	Graphene Oxide
HV	Vickers hardness
MMC	metal matrix composite
MoS_2	Molybdenum disulphide
OM	Optical microscope
S/N	Signal to Noise Ratio
SEM	Scanning electron microscopy
Ti_3SiC_2	Titanium Silicon Carbide
UTM	Universal test machine
XRD	X-ray diffraction
HMMC	Hybrid metal matrix composite
GRCs	The grey relational coefficients

ABSTRACT

Copper, being the second most electrically conductive material, is used in various electrical applications. However, challenges related to mechanical properties, wear resistance. Coefficient of friction and corrosion resistance are still an issue. The aim of this research is to fabricate, characterize, and test copper-based reinforced metal matrix composites in order to investigate and solve different mechanical and tribological properties. The composition was fabricated using stir casting techniques. The casting parameters and weight percentages of reinforcements were selected based on prior reliable research works. As a result, the optimal values for reinforcement composition were determined to be 2-5 wt.%, along with casting parameters of 40 minutes, 430 rpm, 550^0*C, and 1100*^{O}*C for time, stirring speed, preheating and stirring temperature respectively. The addition of reinforcements up to 5 wt.% increased the hardness by up to 194% and compression strength by up to 83%. In addition to the mechanical properties, the tribological properties of coefficient of friction, wear rate, and corrosion rate were minimized to 0.165, 0.09 x 10-8 m3/m, and 0.00073mm/yr respectively. The test result for electrical conductivity demonstrates that there is an inverse relationship between the amount of reinforcement wt.% added and the electrical conductivity. The uniform distribution of reinforcements was observed using scanning electron microscope (SEM) and an optical microscope (OM). The presence of reinforcement nanoparticles was confirmed using X-ray diffraction (XRD). The wear mechanisms of the optimized sample, mainly abrasive and adhesive, were dominant as observed under SEM micrographs. The synergistic effect of reinforcing nanoparticles was observed using FTIR spectroscopy, with the absorption spectra of Si-Compound, C=O, C-OH, and CH showing enhancements in the mechanical and tribological properties of the new composite. The test results demonstrate that the incorporation of* Ti_3SiC_2*-*MoS_2*-GO enhanced both the mechanical properties and tribological properties of the base metal without sacrificing its electrical properties significantly. And it is recommended for use in electrical equipment that requires higher mechanical and tribological properties, specifically for bus bars.*

Keywords: Coefficient of friction; Compression strength; Cu15000-GO/MoS_2/Ti_3SiC_2 composite; Hardness; Stir casting; Wear rate.

CHAPTER ONE

INTRODUCTION

1.1. Background of the Study

A composite is a material made up of two or more than two phases that are produced independently and then joined together to enhance its properties beyond those of its individual components. The manner in which they are combined determines the final material's characteristics. Certain composites offer a combination of strength and lightweight features, making them ideal for various applications, such as car bodies, aircraft components, boat hulls, fishing rods-, and tennis rackets (Groover, 2020).

A composite material is made up of reinforcement incorporated in a matrix of metals, polymers, or ceramics, such as flakes, fibers, particles, or fillers. As it holds the reinforcement together to generate the required shape, the reinforcement improves the mechanical qualities of the matrix. When designed correctly, this combined material exhibits superior property compared to each individual component. Metal matrix composites (MMCs) have emerged as prominent materials, with particular focus on copper MMCs reinforced with particles. These composites have garnered significant attention having to their outstanding mechanical properties (Nee, 2014).

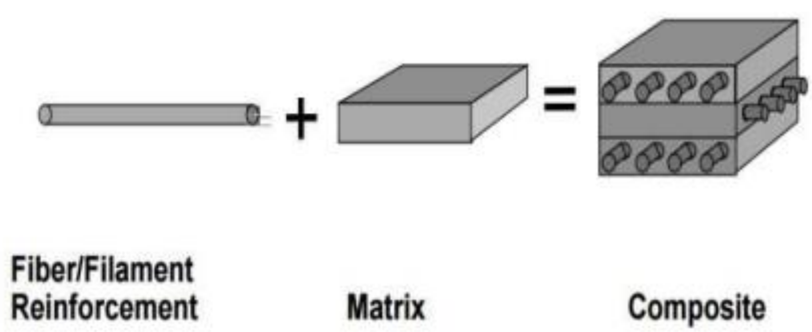

Figure 1.1 Composition of composites (Mishra et al., 2021)

Metal matrix composites, or MMCs, are widely used in a variety of industries, including electronics, aerospace, medical, and automotive. They exhibit remarkable mechanical behaviors like high strength, elevated temperature stability, excellent impact resistance, enhanced fatigue resistance, and high elastic moduli. They also have excellent wear resistance, low ductility, low thermal expansion, good thermal conductivity, and lightweight design, which are all desired qualities. The properties of this materials mainly depends on reinforcement element matrix, and interface (Bansal & Upadhyay, 2016). In MMCs, copper, magnesium, titanium, aluminum and iron They are primarily used as a matrix in combination with SiC, TiC, Al_2O_3, AlN, Si_3N_4,,Y_2O_3, B_4C, ZrO_2,Ti B_2 , etc. for strengthening structures. (Nagavally, 2016).

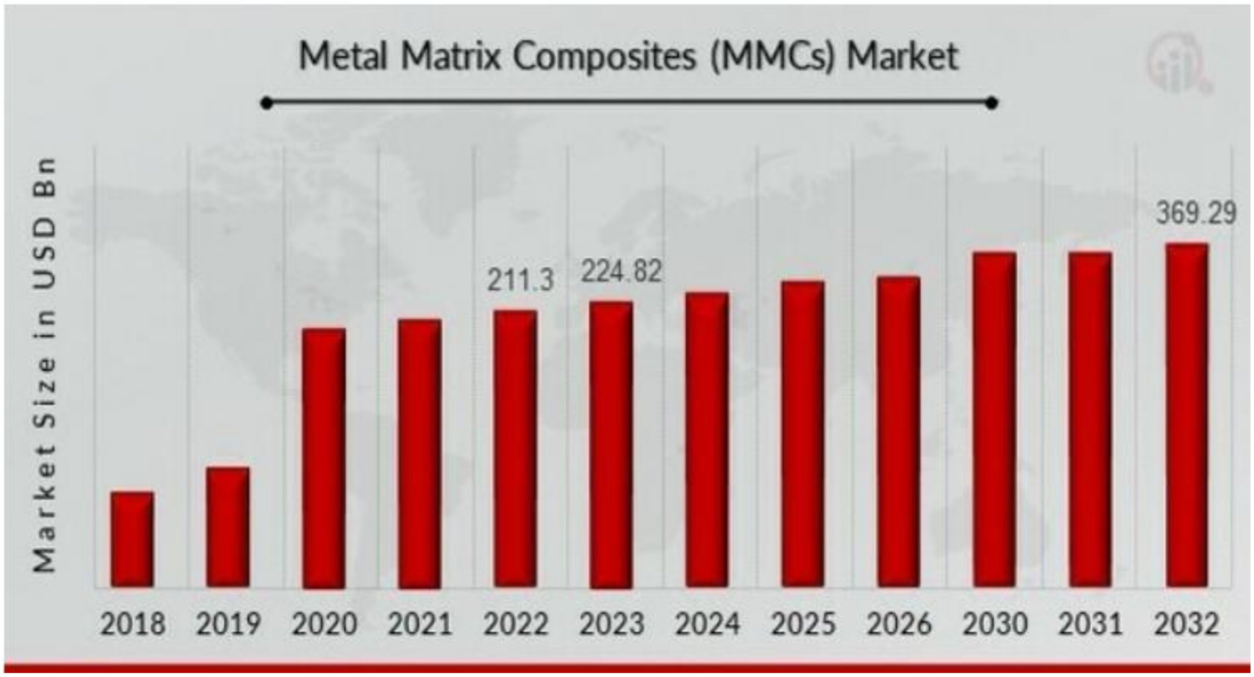

Figure 1.2 Global demands for Metal Matrix Composites (Anshula Mandaokar., 2024)

1.1.1. Copper Metal Matrix Composites

Good temperature resistance, good weldability, high corrosion resistance, and high thermal conductivity are just a few of the many beneficial qualities of copper matrix composites. These properties make them highly promising and sought-after materials for applications in heat exchangers, automobile components, and electrical components (Jamwal et al., 2020).

Copper matrix composites (CMC) are now a days manufactured by various techniques such as liquid metallurgy, powder metallurgy, cold spraying(CS), selective laser melting (SLM), anddiffusion bonding, (Ankur et al., 2021; Huang et al., 2020; Srimurugan et al., 2020; Vairamuthu et al., 2021).

1.1.2. Manufacturing Methods of Metal Matrix Composites

Metal matrix composite is manufactured through liquid phase and solid phase manufacturing methods. In the liquid processing method, the liquid state continuous phase will be generated form discontinuous phase reinforcement, and then the molten metal is cast into the required shape. On the other hand, the solid state manufacturing technique involves creating MMCs under the melting temperature of the matrix (Sharma & Porwal, 2023)**.**

The simplest approach for developing near-net-shaped metal matrix composites is through the liquid metallurgy technique. This method allows for mass production and it is more economical.

The process of stir casting is used to create composite materials. This method involves mechanically stirring a molten matrix metal to combine it with another phase. The goal is to improve the mechanical characteristics of the composites by forging a strong interfacial link between the molten matrix and the dispersed phase. A suitable coating is applied in order to prevent any chemical interactions between the matrix and the dispersed phase. Stir casting is said to be the most affordable and straightforward method for creating liquid composites (Gautam et al., 2018).

1.1.3. MAX Phases

The MAX phase is a viable alternative to ceramic reinforcement and leads to a minimal loss of electrical conductivity in copper-based CMCs. These phases are called Mn+1AXn (where M is an early transition metal, A is an element from the periodic table's columns 13–16, X is either N or C, and n is a number between 1 and 3). These phases make up another class of materials (Jahani et al., 2023).

MAX phases exhibit excellent performance in certain compositions at high temperatures. They possess outstanding oxidation resistance under corrosive conditions up to 1400^{o}C. Additionally, they demonstrate good tolerance to damage and radiation, as well as impressive thermal shock resistance and the ability to heal self-cracks (Gonzalez-Julian, 2021).

1.1.4. Different considerations in the fabrication of metal matrix composites

It is crucial to take into account a number of elements in order to enhance the manufacture of metal matrix composites (MMCs) utilizing the stir casting process. These include optimizing the stirring process parameters, choosing suitable matrix and reinforcement materials, implementing an effective production process, understanding the properties of the metal matrix materials, and addressing related challenges. By focusing on these aspects, the quality of the resulting MMCs can be greatly enhanced. Figure 1.3's cause-and-effect diagram illustrates the different factors to consider when fabricating MMCs.

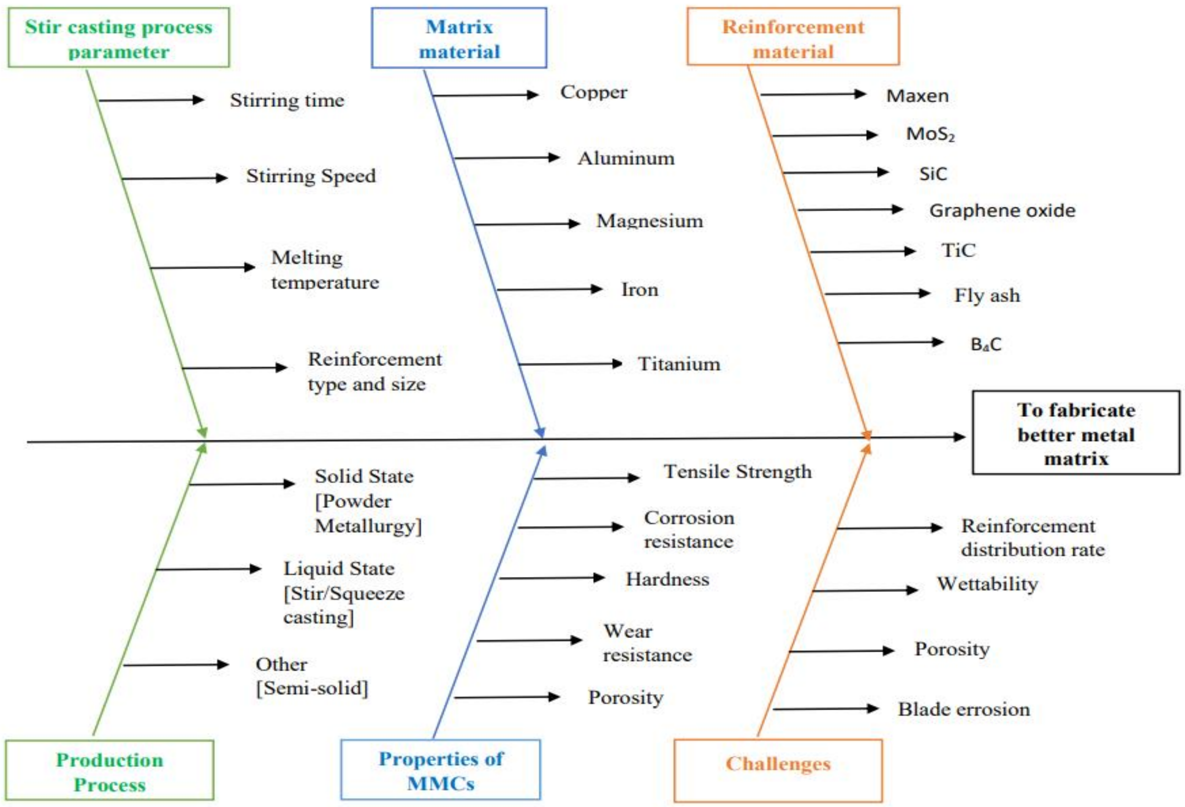

Figure 1.3 Fishbone diagram for improving the quality of fabricated metal matrix composite using stir casting process

Given the information provided, the current research focuses on the development of Cu-MMCs using copper reinforced with MoS2, graphene oxide, and Ti3SiC2 MAX phase particles. It also looks at how the kind of particle affects Cu-MMCs' mechanical characteristics and microstructure. Silicon carbide ceramics were chosen as the reinforcement material due to their numerous exceptional properties, including high strength, high melting point, good thermal conductivity, high hardness, high stiffness, excellent chemical resistance, remarkable wear resistance, and high electrical conductivity. MoS2 is known for its high durability and exceptional chemical and thermal stability, possessing a high melting point and hardness, and also functioning as a lubricant (Abebe Emiru et al., 2023).

1.2. Statement of the problem

Copper is one of the most versatile and highly demanded engineering materials, used in various applications such as electrical equipment, automotive, industrial machinery, and more. Copper matrix composites, which incorporate ceramic particles, are widely recognized for significantly enhancing the thermal expansion behavior, mechanical properties, and high-temperature stability of copper, all while maintaining its high electrical and thermal conductivity. These improvements broaden the scope of copper's applications in thermal and conductive components, including electronic packaging materials, brushes, heat sinks, and integrated circuit lead frames. However, challenges related to wear resistance, ductility, corrosion resistance, and strength-to-weight ratio still persist. Thus, it is crucial for the scientific community to address these challenges and further improve the properties of these alloys, making them suitable for various applications (Nautiyal et al., 2019; Sabzevari et al., 2016; Somani et al., 2018). Although much work has been done to address these issues, further study is needed, particularly on reinforced copper metal matrix composites. Therefore, in order to improve the properties of Cu alloy and address the aforementioned issues, the MAX phase, specifically Ti_3SiC_2, has been proposed. MAX Phases generally has unique properties that combine those of metals and ceramics, such as being strong, electrically and thermally conductive, having remarkable thermal stability, having oxidation resistance, etc. Additionally, MoS_2 and GO are utilized in this study to further enhance the metal matrix's properties and provide a strong wettability impact.

1.3. Research questions

1. What are the main process parameters in the stir casting method?
2. How should the experimental procedure be structured to produce the samples?
3. How can the properties of the samples be measured?
4. How should the optimal, average, and acceptable properties of the samples be determined?

1.4. Objectives

1.4.1. General Objective

The main objective of this research is to Fabricate, Characterize and Test Copper based Reinforced Metal Matrix Composites to investigate different mechanical and Tribological properties.

1.4.2. Specific Objectives

1. To fabricate Copper-based reinforced metal matrix composites using the stir casting method.
2. To determine the effect of the weight percentage of Ti_3SiC_2 on the characteristics of the composite.

3. To investigate Mechanical properties, tribological properties, and microstructural evolution of the samples.
4. To determine the wear morphology of selected sample at specified wear parameters.
5. To determine electrical properties of developed samples.

1.5. Significance of the study

The proposed work is to fabricate MoS_2, Graphene oxide, and Ti_3SiC_2 Max Phase particles reinforced copper composites improve mechanical and tribological properties. Therefore, it has crucial benefits academically and practically to individual and to other stakeholders at national and international level for different industrial applications and as references for further studies. It will enhance theoretical and practical knowledge on research area and for future researcher as a literature and various industrial machinery, roofing, plumbing, transportation and electrical wiring that are in need of this composite material.

1.6. Scope of the Study

The Cu alloy-based composite has been extensively used in the electronic and automotive industries. This research presents a new metal matrix composite designed to address the limitations of current materials. The importance of this study is its potential to improve wear resistance, corrosion resistance in harsh environments, strength-to-weight ratios, creep resistance at high temperatures, and other mechanical properties. Furthermore, it investigates the creation of a uniformly distributed composite that maintains good electrical conductivity and can be produced using a simple, cost-effective method while emphasizing quality.

1.7. Structure of the thesis

This study is structured and organized with well-defined plans to achieve specific objectives. The chapters are outlined as follows: Chapter one provides an introduction that includes the background, problem statement, research questions, objectives, significance, and limitations of the research. Chapter two reviews relevant literature and emphasizing the importance of the study. It examines previous research, highlighting methods and designs, and identifying research gaps. Chapter three describes the materials and methods used in the research. It outlines the experimental procedures, including sample preparation, conducting experiments using Stir Casting, and testing and characterization procedures. The primary focus is to investigate the impact of input process parameters (such as the ratio of matrix and reinforcement, stirring time, stirring speed, and stirring temperature) on the mechanical properties, specifically hardness, compression, density, and porosity of the fabricated MMC samples. Additionally, this chapter discusses the use of the Taguchi-based GRA multi-objective optimization method to determine the optimal sample and covers testing of wear resistance, mechanical properties, and metallurgical analysis (microstructure) of the fabricated samples. The results from various tests are briefly interpreted and discussed, with their implications, limitations, and suggestions for future work addressed. Chapter four presents a comprehensive discussion of the results obtained from different tests. The results are compared and analyzed in relation to the existing evidence presented in the literature review. The findings are interpreted; highlighting their significance and limitations, and the chapter offers insights into potential future research directions. Chapter five concludes the study by summarizing the findings and providing a comparative discussion of the results with the literature review. It offers a concise overview of the study's contributions, implications, and recommendations for further research.

By following this well-structured framework, the study aims to provide a thorough analysis of the subject matter and deliver valuable insights into the fabrication and properties of copper alloy metal matrix composites.

1.8. Limitation for the study

In this study, we will list the constraints that were encountered during the manufacturing of the samples. These include

1. The availability of materials and the willingness of lab organizations to collaborate.
2. The availability and efficiency of machines and facilities for testing and experimentation.
3. Additionally, the installation of machines for specific operations and the need for skilled manpower.

CHAPTER TWO

LITERATURE REVIEW

2.1. Introduction to Composite Materials

A composite is a material structure consisting of at least two distinct materials that work together to achieve enhanced performance. Composite materials are known for their stability and are created by merging two or more different substances, each preserving its unique properties, to form an innovative material with superior characteristics compared to the original materials for specific applications (Gautam et al., 2018).

Composites consist of a combination of two or more elements integrated into a base unit, known as the matrix, which possesses distinct properties. This integration enhances the properties of the base material. Metal matrix composites offer several advantages, including elevated temperature resistance, improved mechanical properties and enhanced electrical conductivity (Madhesh et al., 2020).

2.2. Classification of Composite

Based on the matrix and reinforcing components utilized in their manufacture, composite materials are generally divided into two primary types. They are separated into Carbon Matrix Composites (carbon composites), Ceramic Matrix Composites (CMCs), Metal Matrix Composites (MMCs), and polymer Matrix Composites (PMCs) based on the matrix material, as shown in figure 2.1. Among these, MMCs offer several advantages over other composites. They exhibit excellent resistance to high moisture, temperatures, radiation, and zero outgassing in vacuum environments. Additionally, MMCs provide beneficial electrical and thermal conductivities, along with superior mechanical properties (Arunachalam et al., 2019).

Composite materials may be further classified as fiber-reinforced composites, layer-whisker reinforced composites, and particle-reinforced composites based on the reinforcement, as shown in figure 2.2. Furthermore, composites can be categorized as either organic or inorganic based on their chemical makeup (Yuhazri et al., 2020).

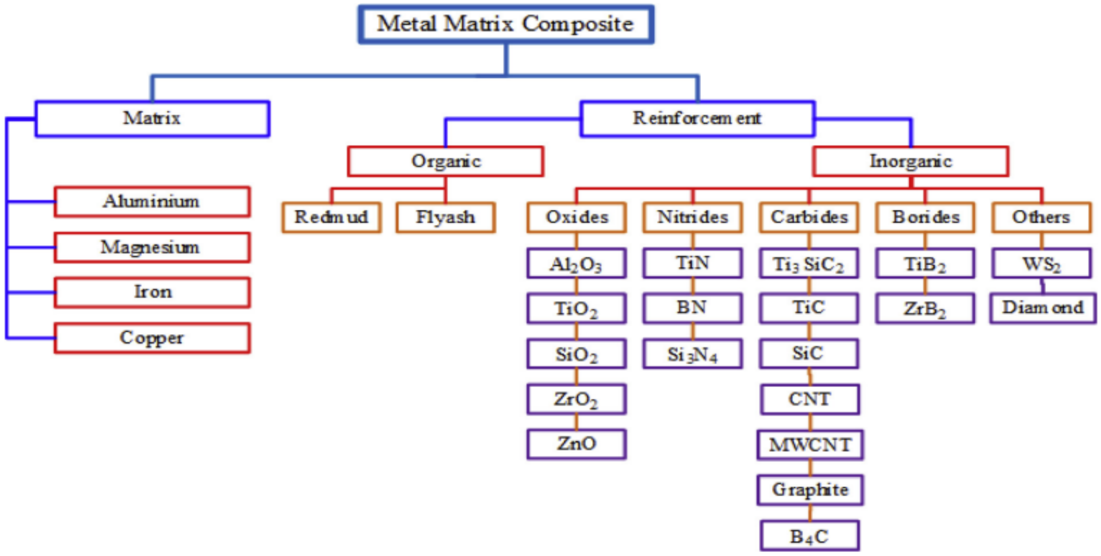

Figure 2.1 Various reinforcement and matrix materials used for the production of MMCs (Arunachalam et al., 2019)

2.2.1. Metal Matrix

Metal matrix composites (MMCs) have evolved as essential engineering materials due to their ability to combine the toughness and ductility of metals with the high elastic modulus and high strength properties of ceramics. MMCs exhibit notable characteristics, including high elastic modulus, resistance to high compressive and tensile stress, and suitability for use at elevated temperatures (Guler & Bagci, 2020).

The matrix material in MMCs is invariably metallic, with commonly used metals being titanium (Ti), magnesium (Mg) Aluminum (Al), and copper (Cu). On the other hand, the reinforcement in MMCs can take the form of dispersed ceramics such as carbides and oxides, or it can be metallic, including materials like lead, molybdenum, or tungsten (Rajak et al., 2019).

2.2.2. Ceramic Matrix

Ceramic whiskers, fibers, and particles are combined to create Ceramic Matrix Composites (CMCs), which are composed of one type of ceramic material encased in another. Strong bonding, usually ionic but occasionally covalent, is a hallmark of these composites. Metals, ceramics, polymers, or other materials can be used to strengthen the ceramic matrix in CMCs. enhanced qualities such as enhanced corrosion resistance, compressive strength, stability at high temperatures, and high melting points are offered by ceramic-based matrix materials. Due to these attributes, ceramic matrices are commonly employed in high-temperature applications, including rotors, blades, and pistons in gas turbine components. They can withstand corrosive environment and operate effectively in high temperatures, making them a preferred choice (Sharma et al., 2019).

2.2.3. Polymer Matrix

Polymers are materials that can be found naturally or synthesized artificially, characterized by long chains of molecules arranged in a three-dimensional structure. They possess remarkable flexibility and strength. By incorporating specific reinforcements into the polymer matrix, known as polymer matrix composites, their physical and chemical properties can be further enhanced. This advancement has revolutionized industries such as aerospace and automobile, as these composites offer entirely new properties and capabilities **(**Chohan et al., 2022).

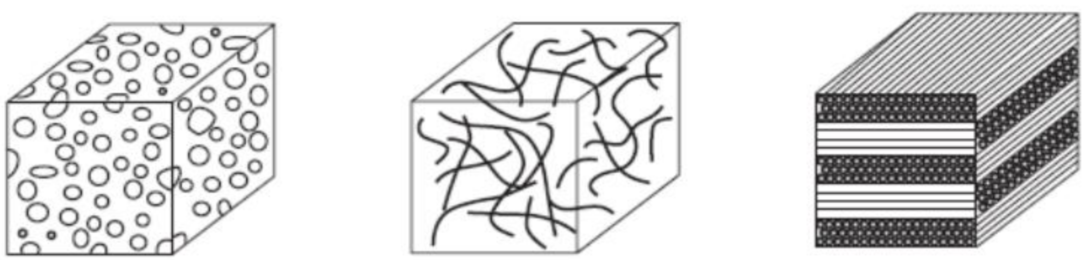

Figure 2.2 Geometries of composite materials reinforcement: (a) particulate composites, (b) fiber composites, and (c) layer-whisker composites (Yuhazri et al., 2020)

2.2.4. Particulate

Comparatively speaking, fiber-based composites are more successful in strengthening than particle-based composites. Particle-reinforced composites, however, are appropriate for uses like road surfaces that demand high levels of wear resistance. Particle-reinforced composites have several benefits, including low cost and simplicity of manufacture and shaping. Concrete is a perfect illustration of a particle-reinforced composite, with coarse rock fragments incorporated in a cement matrix. In this case, the cement serves as a binder to keep the structure together while the aggregates provide it strength and rigidity.

When utilizing a large volume proportion of glassy particles based on iron as reinforcement in an aluminum matrix, Metal Matrix Composites (MMCs) experience a considerable hardening of the matrix. As a consequence, the composite material has an amazing blend of high strength and plasticity **(**Rajak et al., 2019).

2.2.5. Fiber

Fiber-reinforced materials make up a significant portion of composite materials and they are extensively utilized. These materials offer exceptional characteristics, including high specific strength, low specific gravity, and high specific modulus. These properties effectively enhance the rigidity, tensile strength, and dimensional stability of the composite material. Additionally, fiber reinforcement can increase low-temperature impact strength and the heat-distortion temperature.

Fiber composites consist of a higher amount of independent fibers, typically ranging from several thousand to tens of thousands per square centimeter. These fibers are bound together by a tough matrix. When a few fibers experience failure due to overload or other factors, the load is redistributed to the remaining unbroken fibers. This prevents sudden catastrophic failure of the components over a short period of time, enhancing the overall durability and damage tolerance of the composite material (Yang et al., 2019).

Fiber-based composite materials have garnered significant attention due to their lightweight nature, corrosion resistance, durability and high strength. By functionalizing the fiber materials, composite materials can maintain their natural properties while also improving or overcoming the weaknesses of individual materials (Yang et al., 2019).

2.2.6. Layer-whisker

Single crystals are cultivated with minimal defects and often take the form of discontinuous and short fibers with varying cross sections. These fibers are crafted from materials such as silicon carbide, graphite, iron, copper, and others. Their typical lengths fall within the range of 3 to 55 nanometers (Kashyap, 2019).

2.2.7. Copper Metal Matrix

Cu-MMCs consist primarily of a matrix, and lubricant components, with the latter being crucial for handling a high coefficient of friction (COF) and supporting loads in copper metal matrix composites. These components significantly impact the tribological performance of the metal matrix, especially in demanding braking conditions. As a result, the development and analysis of abrasion components and their performance characteristics can offer valuable insights for enhancing the design and production of high-performance Cu-MMCs (Zhou et al., 2023).

The evolution of metal matrix composites (MMCs) with whiskers and continuous fibers as reinforcements began in the 1970s, leading to breakthroughs in high-performance applications. Composite materials comprise different materials with distinct chemical and physical properties. When integrated, these materials give a composite with a wide range of properties. Although composite materials are heterogeneous on a microscopic scale, they exhibit homogeneity on a macroscopic scale (Gill et al., 2022).

Reinforcements are utilized in copper matrices, particularly in hybrid composites. Successful fabrication methods include stir casting and powder metallurgy. Increasing the proportion of reinforcements can result in higher porosity, while density varies with the density of the reinforcements. Reinforcements enhance the strength of the composite material in terms of tensile, compressive, impact, fatigue, as well as surface properties such as corrosion and wear. Further improvements can be explored through processes like surface alloying, melting, and heat treatment via laser processing (Suman et al., 2021).

2.2.8. MAX Phase

A class of ternary carbide compounds known as MAX phases has attracted a lot of interest because of its special set of characteristics. These properties make them highly suitable for use in extreme conditions, such as high temperatures and aggressive environments. Similar to metals, MAX phases exhibit excellent electrical and thermal conductivity, as well as favorable processing properties. They are ductile, relatively soft, and resistant to thermal shocks. Conversely, MAX phases also possess ceramic-like characteristics. They are refractory, resistant to oxidation, and exhibit high tensile strength, a high melting point, and good thermal stability. These attributes make them promising materials for various applications, including those in the aerospace industry. The general formula for MAX phases of carbide compounds is Mn+1AXn, where n can be 1, 2, or 3. From this, M represents a transition metal (typically titanium or chromium), A predominantly denotes a Group IIIA or IVA element, and X signifies carbon. Structurally, these compounds consist of alternating layers of Mn + 1Xn and A atoms, with carbon atoms occupying octahedral sites between the M atoms (Gorshkov et al., 2017).

MAX phases are often referred to as metallic ceramics because of their remarkable blend of ceramic and metallic properties. They exhibit excellent thermal and electrical conductivity, damage tolerance, resistance to machinability and thermal shock, similar to metals. At the same time, they possess ceramic properties such as being lightweight, resistant to elastically rigid, and oxidation (Hadi et al., 2019). Some compositions of MAX phases show exceptional performance at high temperatures, including outstanding oxidation resistance up to 1400 °C in corrosive environments, good radiation and damage tolerance, self-crack healing and thermal shock resistance (Gonzalez-Julian, 2021).

Cu-based composites reinforced with Ti_3SiC_2 reinforced are considered a promising material for electrical contacts. The adhesion strength between the Cu matrix and Ti_3SiC_2 depends on the interfacial properties of the composite (Xiong et al., 2021).

Achieving superior high electrical conductivity and mechanical properties in ceramic/metal composites is of significant importance. Plasma spraying was employed to prepare Cu/Ti3SiC2 composite coatings with 20 and 50 wt.% Ti3SiC2. The mechanical properties, microstructure, tribological properties, and electrical conductivity of the coating were investigated. The results revealed the presence of primary compound regions, as well as decomposition and diffusion zones within the coatings. The 20 wt% Cu/Ti3SiC2 composite coating exhibited a denser microstructure and the highest micro hardness of 224 HV0.1, while the 50 wt% Cu/Ti3SiC2 coating showed higher fracture toughness (1.26 MPa•m1/2). Additionally, both the 20 and 50 wt% Ti3SiC2/Cu composite coatings demonstrated significantly high electrical conductivity, with values of 7.9 and 4.3 × 10^6 S/m, respectively (Yang et al., 2023).

2.2.9. MOS_2

(Zhang et al., 2015) carried out a work wherein a hydrothermal technique was used to produce a hybrid material, MoS2/reduced graphene oxide (MoS2/RGO). Then, using a powder metallurgy process, Fe-Ni matrix composites were created with different weight fractions of MoS2/RGO

(1%, 3%, 5%, and 7%). Using a ball-on-plate wear and friction tester, the tribological characteristics of these composites were examined at temperatures between room temperature and 600°C. The crumpled RGO sheets had a strong bond with the MoS2 nanospheres, which are composed of petal-shaped nanosheets, according to the results. Over a broad temperature range, the Fe-Ni matrix composites with an acceptable RGO/MoS2 concentration demonstrated outstanding anti-wear capabilities and friction reduction. The tribological performance of the composites was greatly enhanced by the RGO in the RGO/MoS2 hybrid material.Notably, the specimen with 3 weight percent RGO/MoS2 showed the lowest friction coefficient (0.21) and the most steady wear rate (1.07–1.90 x 10^-5 mm^3/Nm). It was found that the lubricating action of sulfide films and the glaze layer generated on the friction surface at high temperatures were responsible for the wear rate of 1.07 x 10^-5 mm^3/Nm and the friction coefficient remaining below 0.30 at 600°C. The composites' exceptional tribological performance resulted from the combination of high hardness and solid lubricants working in concert.

We looked at how the MoS2 presence affected the pure copper's microstructure, hardness, density, and wear resistance. By physically grinding and hot pressing pure copper and MoS2 powders, with MoS2 particles varying in mass from 0% to 10%, copper-based composites were produced. Utilizing a pin-on-disk configuration and a constant sliding speed of 0.2 m/s, the wear resistance was assessed in dry sliding circumstances. Hardness testing revealed that the greatest hardness was achieved at a critical MoS_2 level of 2.5%. Regardless of the applied normal load, the $Cu/2.5MoS_2$ composite showed the lowest wear loss and coefficient of friction. Wear volume rose with increasing normal load, however the coefficient of friction reduced as the applied normal load increased from 1 to 4 N at any reinforcement content. Images captured by scanning electron microscopy (SEM) of the worn surfaces and debris revealed a change in the wear process in Cu/MoS_2 composites, which is now largely a mix of abrasion and delamination, as opposed to adhesion in pure copper (moazami-goudarzi & nemati, 2018).

2.2.10. Graphene oxide

The average grain size was around 0.26 μm under the ideal preparation circumstances, which included employing a GO concentration of 0.8 g/L and 120 W ultrasonic power in the plating solution. The combination showed a strong crystallographic orientation of (220) because to its lower grain size. Furthermore, the GO concentration in the composites grew from 0.67 wt% to

1.72 wt% as a result of the ultrasonic treatment, and it was uniformly distributed throughout the composite foil. The Cu/GO composite foil exhibited notable enhancements in several characteristics in contrast to pure copper foil. There was less friction as evidenced by the average friction coefficient falling from 0.87 to 0.72. In addition, the composite foil's hardness rating almost doubled to 74.6 HV0.1. The composite foil's tensile strength increased to 239 MPa along with a 17% elongation. Furthermore, in optimal circumstances, the thermal conductivity rose to 556.57 W m^{-1} K^{-1}, a 39.8% increase. Three main elements are responsible for these improvements in the GO/Cu composite foil's thermal mechanical properties: a modification in the preferred orientation, grain refinement, and the existence of decreased GO reinforcement that forms a network within the foil (Zhan et al., 2023).

2.3. Manufacturing technology of metal matrix

Different processing or fabrication methods can be utilized for matrix material and reinforcement material based on their specific characteristics. These methods can be applied to process these materials in solid, liquid, and gas states. Recent advancements in the field have introduced new techniques for processing Metal Matrix Composites (MMCs), such as rapid prototyping, spark plasma sintering, laser sintering, and more (Sankhla & Patel, 2022).

2.3.1. Solid State Processing

There are several ways available for producing Metal Matrix Composites (MMCs) using solid-state processing processes. Among these techniques are friction stir processing, cold spraying, spark plasma sintering, high energy ball milling, powder metallurgy, diffusion bonding, and cold spraying. Fine powders are combined, compressed into the required shape, degassed under vacuum, and then sintered in a regulated environment in the powder metallurgy process. Producing intricately formed precision parts with superior mechanical and structural qualities and high uniformity is a specialization of this method.

There are several ways available for producing Metal Matrix Composites (MMCs) using solid-state processing processes. Among these techniques are friction stir processing, cold spraying, spark plasma sintering, high energy ball milling, powder metallurgy, diffusion bonding, and cold spraying. Fine powders are combined, compressed into the required shape, degassed under vacuum, and then sintered in a regulated environment in the powder metallurgy process.

Producing intricately formed precision parts with superior mechanical and structural qualities and high uniformity is a specialization of this method (D. Kumar et al., 2019).

2.3.2. Liquid State Processing

Metal Matrix Composites (MMCs) with intricate geometries may be fabricated using liquid-state processing techniques, which also provide reasonably priced options. Excellent dispersion and good interfacial stirring are made possible by these techniques, which lead to homogenous reinforcement phase distribution and improved bonding. A few well-known liquid-state processing methods that improve mechanical characteristics include squeeze casting, casting, and infiltration (Abbas et al., 2021).

The next section will focus on one of the conventional methods for processing metal matrix composites, which is called as stir casting.

2.4. Stir Casting

Metal Matrix Composites (MMCs) with intricate geometries may be fabricated using liquid-state processing techniques, which also provide reasonably priced options. Excellent dispersion and good interfacial stirring are made possible by these techniques, which lead to homogenous reinforcement phase distribution and improved bonding. A few well-known liquid-state processing methods that improve mechanical characteristics include squeeze casting, casting, and infiltration.

The introduction part covered many ways in short to provide readers interested in MMC manufacturing procedures a good foundation. After a thorough analysis of the literature, with an emphasis on the mechanical characteristics of the manufactured MMCs, the review came to the conclusion that the best configuration for producing MMCs is a bottom tapping stir casting furnace with electromagnetic and ultrasonic stirrers as well as a squeeze attachment. (Arunachalam et al., 2019).

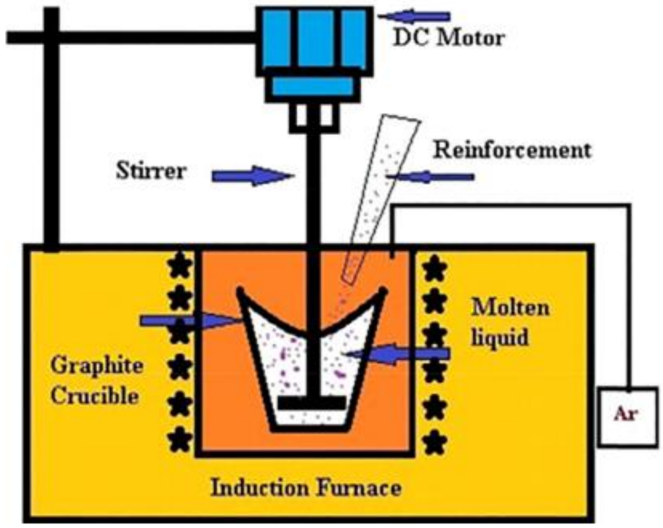

Figure 2.3 Schematic diagram of the stir casting setup (Madhukar et al., 2019)

2.4.1. Stir casting Parameter

The stir casting method was used to produce a Copper Metal Matrix Composites (MMCs). Different sizes of TiC (Titanium Carbide) particles were utilized in the fabrication process, with varying weight percentages of 2%, 4%, and 6%. It was observed that the properties of the composite material decreased when the TiC content exceeded 6% in the copper MMC.

During the fabrication process, the stirrer time was also varied, with durations of 30, 40, and 50 minutes. The pure copper was placed inside a muffle furnace and heated to 1100°C. The titanium carbide particles were preheated separately to 800°C for duration of 50 minutes. The purpose of preheating was twofold: to remove any moisture and oxidation from the particles and to enhance the material properties by strengthening them (Vairamuthu et al., 2021).

Table 2.1 An overview of the different techniques used for damage to reinforcement MMC fabrication (N. Kumar & Kumar, 2023)

Method	Ranges of shape and size	Metal yield	Range of vol. fraction	Damage to reinforcement	Cost
Liquid Metallurgy (Stir casting)	Wide range of shapes, larger size up to 500Kg	Very high (>90%)	Up to 0.3	No damage	Least expensive
Squeeze casting	Limited by preform shapes, up to 2cm height	low	Up to 0.45	Several damage	Moderately expensive
Powder metallurgy	Wide range, restricted size	High	-	Reinforcement fracture	Expensive
Spray casting	Limited shapes, large size	Medium	0.3-0.7	-	Expensive
Lanxide technique	Limited by preform shapes, restricted size	-	-	-	Expensive

2.5. Application of Metal Matrix Composite

Enhancing the properties of contact materials used in electrical switches is a crucial task in materials engineering for efficient power management systems. The applications and principles of electrical contacts have been extensively discussed. It was found that two main materials are preferred for high-power electrical switching contacts.

The first material is silver and its compounds, which are chosen for their low contact resistance and high conductivity. The second material is copper, which serves as a good and more cost-effective alternative for electrical contacts. Because copper and its compounds tend to oxidize when exposed to air, they are usually employed in an inert environment. At the contact interface, oxidation causes an increase in contact resistance and a decrease in electrical conductivity.

Various materials are applied to copper and silver surfaces to change their characteristics, particularly their hardness and behavior under electrical arcing circumstances. This may entail using composite materials that incorporate ceramic particles or forming alloys by adding other metals. The impact of alloying or composite production on the electrical conductivity and hardness of contact materials is depicted in Figure 2.3. Hardness rises and electrical conductivity falls as the amount of second phase material increases. Nonetheless, since the combination of these actions greatly increases the lifespan of certain contact materials, it is generally acknowledged..

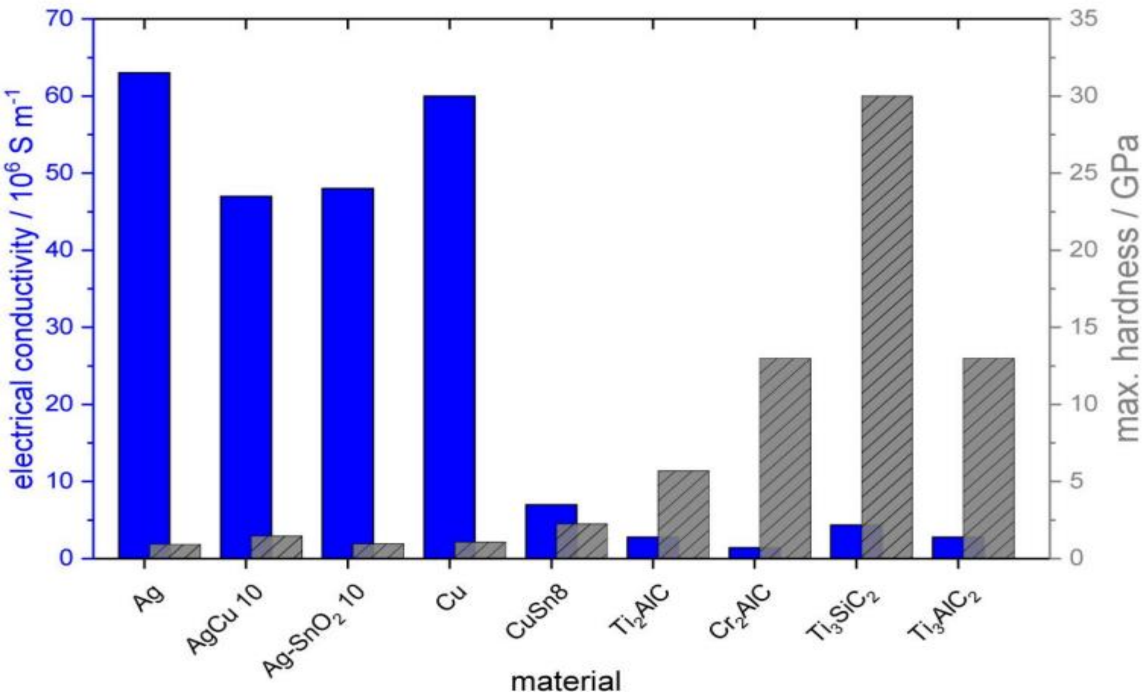

Figure 2.4 Influence on the hardness and the electrical conductivity of silver and copper by alloying or formation of composites compared to Mn+1AXn phase materials (Grieseler et al., 2017)

2.6. Recent Research Developments on Copper Matrix Composites

This section comprehensively analyzes previous research on copper matrix composites (CuMCs), specifically focusing on Cu15000. It explores two subsections: hybrid-reinforced copper matrix composites and single-reinforced copper matrix composites. The research discusses the findings of mechanical characteristics (compression, tensile, and hardness tests), tribological tests (wear and corrosion), as well as electrical and thermal tests. Additionally, investigations were conducted to examine the effects of adjusting the weight percentage of different reinforcements in copper metal matrix composites.

2.6.1. Manufacturing of Copper Composite using stir casting

(Arunachalam et al. 2019) carried out a thorough analysis of the stir casting process, including important facets like the characteristics of the composite, furnace design, manufacturing difficulties, and research potential. The review is made more original by the authors' insightful recommendations about furnace design, reinforcement and matrix material selection, additives, and process parameters. The article briefly covers many ways in the introductory section to provide readers a baseline understanding of MMC production procedures. Based on a critical analysis of the literature, with a focus on the mechanical and tribological behaviors of produced MMCs, the authors suggest using a squeeze attachment along with ultrasonic and electromagnetic stirrers equipped with a bottom tapping stir casting furnace for MMC production.

2.6.2. MAX Phase reinforced Copper Composite

(Grieseler et al. 2017) prepared a composite coating system using MAX phase particles (Ti_2AlC and Ti_3AlC_2) and copper through direct current electrode position. It was successful to add micro-scale MAX phase particles (up to 3 weight percent) to the copper coating, which produced a uniformly dispersed composite. The study examined variations in coating characteristics in layers around 50 µm thick, such as electrical contact resistance, hardness, and crystalline structure. Additionally examined were the characteristics of the composite coatings in electrical arcing scenarios. The findings showed increased hardness and slight structural changes due to particle incorporation. The electrical contact resistance of the composite coatings was same with pure copper films deposited under the similar conditions. Notably, the composite coatings exhibited improved performance under electrical arcing compared to pure copper layers, which showed recrystallization melting. These composite layers show potential for electrical applications, precisely in electrical switching devices.

(Suman et al. 2021) investigated the use of reinforcements in copper matrices, particularly hybrid composites. Successful fabrication methods included stir casting and powder metallurgy. The proportion of reinforcements influenced porosity, while density varied with the density of the reinforcements. The inclusion of reinforcements enhanced surface properties (wear, corrosion) and the strength (tensile, compressive, impact, fatigue) of the composites. Future improvements can be explored through processes like heat treatment, alloying via laser processing and surface melting.

2.6.3. Mechanical and Tribological Properties of Copper Composite

In a 0.1 M NaCl solution, it was found that Cu-HSSS-WC hybrid composites had better mechanical behavior and corrosion resistance qualities. Three different kinds of composites with different HSSS contents were created in strip form via stir casting (A1-1%, A2-2%, and A4-4%). Characterization was accomplished using energy dispersive X-ray analysis, scanning electron microscopy, X-ray diffraction, and microstructure analysis. Tafel polarization curves and alternating current impedance measurements were used to assess the corrosion resistance of the composites, and the results showed that A4 > A2 > A1. This ranking was in line with the order established by final tensile strength and hardness measurements (M. K. Singh et al., 2019).

Reduced graphene oxide (rGO)/copper composites were developed to enhance the mechanical and tribological capabilities of copper while mostly maintaining its physical attributes. Adding 0.5 wt% of nanocomposite to copper decreased the coefficient of friction by an impressive 77.5% compared to pure copper. Furthermore, reinforcing copper with 0.75 wt% of nanocomposite increased its flexural strength by 15.2%, while the modulus of 1 wt% of nanocomposite reinforced copper experienced a 31.3% increase. The notable decrease in the coefficient of friction in the composites was a result of the addition of thin rGO films to the worn track as well as the improved hardness and strength of the material. The physical characteristics of the composites, such as their electrical and thermal conductivities, gradually decreased as the amount of reinforcement rose. The efficient dispersion of rGO in the copper matrix was achieved by the two-step composite production method, producing a composite with constant characteristics throughout (Pratik et al., 2020)

2.6.4. Electrical Properties of Copper Composite

(Salvo et al. 2019) examined the connection between Cu-graphene composites' electrical conductivity and hardness at different sintering temperatures. When compared to pure Cu solidified at 600°C, they found that 1% Cu reinforced with graphene improved electrical conductivity by around 22%.

(Song et al. 2024used hot-press sintering of Cu-Al_2O_3 powders, where the graphene was produced in-situ on an internal oxidation layer, to combine Al_2O_3 and graphene particles into a Cu matrix. With an ultimate tensile strength of 600 MPa and an electrical conductivity of 81.7% IACS, this composite demonstrated a desirable combination of conductivity and strength, which was attributable to the cooperative action of Al_2O_3 and graphene particles.

(Nazeer et al. 2019) aimed at improving the decreased graphene oxide/metal composites' anisotropic hardness and thermal conductivity. They used powder metallurgy to create copper-graphite and copper-reduced graphene oxide composites. X-ray diffraction (XRD), Raman spectroscopy, scanning electron microscopy (SEM), and X-ray photoelectron spectroscopy (XPS) were among the methods used to analyze the composites. The findings demonstrated that an anisotropic thermal conductivity ratio of 1.68 and a hardness of 71.2 HV were attained by a copper-reduced graphene oxide composite with a mesh size of 3500 μm and 1 weight percent graphene oxide. These values represented improvements of 80% and 61% over pure copper, respectively. The use of a mesh size of 3500 μm for graphite and graphene oxide yielded superior results compared to smaller mesh sizes. These composites demonstrate promising potential as heat sink materials in thermal packaging applications.

Table 2.2 Summary of Hybrid-reinforced copper composite

Authors	**Title**	**Their work**	**Result**
Gautam, Y. K., Somani, N., Kumar, M., & Sharma, S. K. (2018).	A review on fabrication and characterization of copper metal matrix composite (CMMC)	Cu is reinforced using SiC using powder metallurgy, Up to 20% of SiC is incorporated	Increased up to 90HV Tensile strength more 250MPa Improvement in corrosion resistance
Mohan, E., Anbuchezhiyan, G., Pugazhenthi, R., & Prakash, F. P. (2023).	Wear behavior of brass based composite reinforced with SiC and produced by stir casting process	Silicon carbide-reinforced brass-based composite were synthesized by stir casting.	The wear rate varied from 0.0135 to 0.0893 mm3/min
Shaik, M. A., & Golla, B. R. (2020).	Mechanical, tribological and electrical properties of ZrB2 reinforced Cu processed via milling and high-pressure hot pressing	ZrB2/Cu composites were fabricated by high pressure hot press up to 1owt% of ZrB2 was used	Hardness and compressive strength increment up to 121% and 93% wear rate (from 49.3 × 10-3 mm3/Nm to 9.1 × 10-3 mm3/Nm) Cu–ZrB2 samples decreased from 75.7% IACS to 44.1% IACS
Singh, M. K., Gautam, R. K., & Ji, G. (2019).	Mechanical properties and corrosion behavior of copper based hybrid composites synthesized by stir casting.	Three types of Cu-HSSS-WC hybrid composites, having different quantity of HSSS (A1-1%, A2-2% and A4-4%), are prepared by stir casting	Increase 55% in hardness result Increment of UTS result up to 430MPa Improvement in corrosion resistance
Somani, N., Tyagi, Y. K., Kumar, P., Srivastava, V., & Bhowmick, H. (2018).	Enhanced tribological properties of SiC reinforced copper metal matrix composites.	The composite samples Cu - SiC were prepared by powder metallurgy technique with SiC = 10, 15 and 20% volume fraction of SiC.	The hardness and tensile strength of the samples was found to increase by 48% and 24% respectively by adding 20% of SiC Wear is reduced from 45% to 77%, whereas friction reduced to 25% to 44%, due to the addition of SiC from 10% to 20% respectively
Yehia, H. M., Ali, A. I., & Abd-Elhameed, E. (2023)	Effect of exfoliated MoS2 on the microstructure, hardness, and tribological properties of copper matrix nanocomposite fabricated via the hot pressing method.	Pure copper, copper with 10% alumina, and copper with a mixture of alumina and molybdenum disulfide in a ratio of 1:1 (Cu, Cu/10 Al2O3, and Cu/ hybrid (10 Al2O3-10 MoS2)) was prepared	The copper sample reinforced with the hybrid of alumina/MoS2 gave the lowest mechanical wear rate and the lowest average friction coefficient of 0.17

2.7. Research gap

The literature review indicates that considerable research has been conducted on the synthesis, characterization, and testing of copper metal matrix composites (MMCs) using ceramics for general applications. However, there is still gap on the studies focusing on the development of copper MMCs reinforced with MAX phase materials. To address this research gap, the proposed work aims to fabricate Copper metal matrix composites reinforced with MAX phase materials and comprehensively evaluate their mechanical, metallurgical, tribological, and electrical properties.

CHAPTER THREE

MATERIALS AND METHODOLOGY

The proposed work has been aimed at Fabrication of Copper based Reinforced with GO/MoS_2/Ti_3SiC_2 MAX Phase. The objective of this research is to Fabricate, Characterize and Test Copper based Reinforced Metal Matrix Composites to investigate different mechanical and tribological properties.

Materials that are to be used on this research work are metal matrix (copper alloy) and reinforcement matrix of MoS_2, graphene oxide, and Max phase that yields the needed properties and small amount of molybdenum disulfide will be used for self-lubrication properties. The synthesis of material will be carried out through stir casting process at different weight composition of reinforcement materials with uniform particle size. Addition of Molybdenum disulphide (MoS_2) and Graphene oxide is fixed which is used to improve the wettability between liquid matrix and MXene reinforcement. The effect of weight composition of the reinforcement materials on density, porosity, hardness, compression strength, wear and corrosion resistance of Cu-MMCs will be studied and reported. Microstructure analysis will be carried out on each of casted composites using SEM to know fair distribution and clarify porosity.

The mechanical property such as hardness test and compression strength test, tribological tests such as wear and corrosion resistance as well as microstructural studies will be carried out as per ASTM standards.

The evaluation is based on the standard test code of ASTM E92-72, ASTM G99, and ASTM E9, for hardness test, wear test, Compression test, respectively will be used. Therefore, the samples size, dimension and volume will depend on their ASTM test standard.

3.1. Matrix reinforcements

The materials utilized in this work to create the hybrid copper composite include molybdenum disulfide (MoS2), graphene oxide (GO), MAX phase (Ti_3SiC_2), and copper alloy (C15000), which serves as the basis material. Cu 15000 was selected because of its better and higher electrical conductivity than commercially available Cu-Br, Cu-Cr, and Cu-Nb alloys (Muramatsu et al., 2013). Table 3.1 lists the grams of each item that are required.

Table 3.1 The materials required in kg to develop hybrid Cu15000 matrix composite

No.	Item	Quantity(g)
1	Copper alloy (Cu15000)	2145
2	MAX Phase/Ti_3SiC_2/	117.6
3	Graphene oxide/GO/	58.8
4	Molybdenum disulfide /MoS_2/	58.8

3.1.1. Matrix

Matrix is one part of composite materials, which is utilized in order to carry load to and between reinforcements, bind reinforcements together via its cohesive and adhesive capabilities, and shield reinforcements from external factors including humidity and chemical attacks. As was covered in the earlier chapters, composites are divided into the following three categories depending the kind of matrix material: ceramic matrix composites (cMCs), polymer matrix composites (CMCs), and metal matrix composites (MMCs). Because of its fundamental advantages over PMCs and CMCs, MMCs are the composites that are used in the industrial sectors to the greatest extent (Guler & Bagci, 2020; Rajak et al., 2019). In this work, hybrid metal matrix composites (HMMC) are made using copper alloy (Cu15000) as the matrix material.

3.1.1.1. Copper Alloy (Cu15000)

As mentioned in the introductory part of chapter one, the creation of MMCs involves the use of a variety of matrix materials, including copper, aluminum, magnesium, and other metals. Copper is a highly preferred matrix material due to its superior density, strong heat and electrical conductivity, and resistance to corrosion, making it one of those metals.

As shown in Table 3.2 and 3.3, Copper Zirconium has ductile, corrosion resistant, very high thermal and electrical conductive characteristics. Its density 8.89 g/cm3 (0.324 lb/in^3), which is relatively denser, and it is composed of copper and zirconium.

Copper alloy bars which are used as a matrix material in the fabrication of hybrid composites are illustrated in Figure 3.1 below.

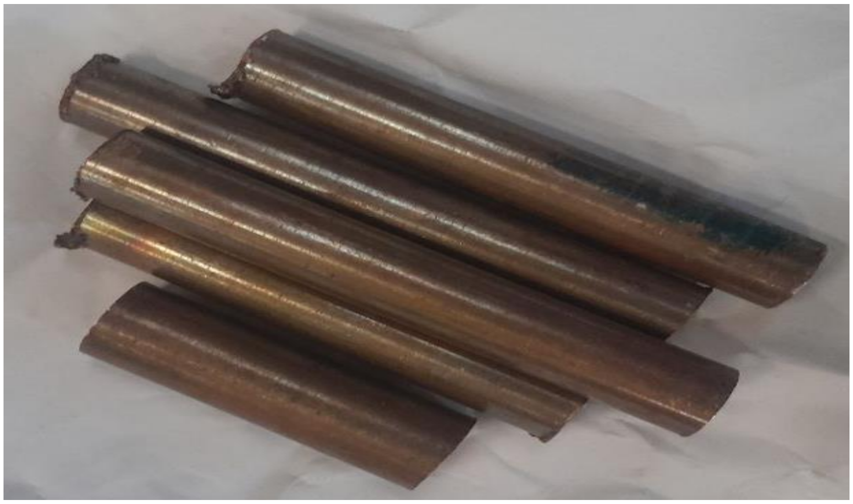

Figure 3.1 Copper Zirconium bar

Table 3.2 Summary of physical and mechanical properties for Copper

Physical and Mechanical properties	Metric	Unit
Density	8.89	g/cm3
Ultimate Tensile Strength	430	MP
Compressive strength	295	MP
Thermal conductivity	367	$Wm^{-1} K^{-1}$
Electrical conductivity (Sm−1)	54.95	Sm^{-1}
Modulus of Elasticity	110	GPa
Shear Modulus	46	GPa
Hardness	129	HV

Table 3.3 Chemical composition of UNS C15000 Copper Zirconium

Element	Cu	Zr
Content (%)	99.8-99.9	0.1-0.2

3.1.2. Reinforcements

The reason the phase is named reinforcement is because it is stronger than the matrix phase. As a result, reinforcements provide composites their stiffness, strength, and thermal stability, among other structural qualities. The following qualities are commonly thought to be present in the reinforcing phase (reinforcement): good process ability, low wear resistance, high compression, high tensile strength, high Young's modulus, and good chemical and mechanical compatibility.

This study focuses on utilizing MAX phase (Ti_3SiC_2), Graphene oxide (GO), and Molybdenum disulfide (MoS_2) as reinforcement materials to create a hybrid composite with a Copper alloy matrix. The properties and composition of each of these reinforcements are discussed below.

3.1.2.1. MAX phase- Ti_3SiC_2

Due to their mixed atomic bonding, MAX phases combine the mechanical robustness of metals with the oxidation and thermal resistance of ceramics, offering considerable promise for high-stress and high-temperature applications. Because of its exceptional mix of characteristics, the ternary carbide Ti3SiC2 is one of the most promising MAX phases for high temperature applications. Ti3SiC2 has an excellent compression strength of 1100 MPa, a high Young's modulus of 400 GPa, and a density of 4.5 g/cm3. Additionally, bulk Ti3SiC2 materials have outstanding oxidation and wear resistance as well as self-healing processes at high temperatures, all without sacrificing their electrical and thermal conductivities (Yang et al., 2023). Table 3.4 and 3.5 illustrate the properties and composition of Ti_3SiC_2. And Figure 3.2 present the Ti_3SiC_2 used for the research.

Table 3.4 Physical and Mechanical properties of Ti_3SiC_2 MAX

Mechanical property	Metric	Unit
Density	4.5	g cm^{-1}
Tensile Strength	200	GPa
Compressive Strength	1100	GPa
Modulus of Rapture	400	GPa
Young’s Modulus	300	GPa
Electrical Conductivity	4.5×10^{6}	$\Omega^{-1}.m^{-1}$
Thermal Conductivity	37	W/m.K
Co-Efficient of Thermal Expansion	9×10^{-1}	$^{o}C^{-1}$

Table 3.5 Chemical composition of Ti_3SiC_2

Element	Ti	Si	C
Content wt.%	48.4 $\pm$ 0.6	19.4 $\pm$ 2.4	32.2 $\pm$ 1.8

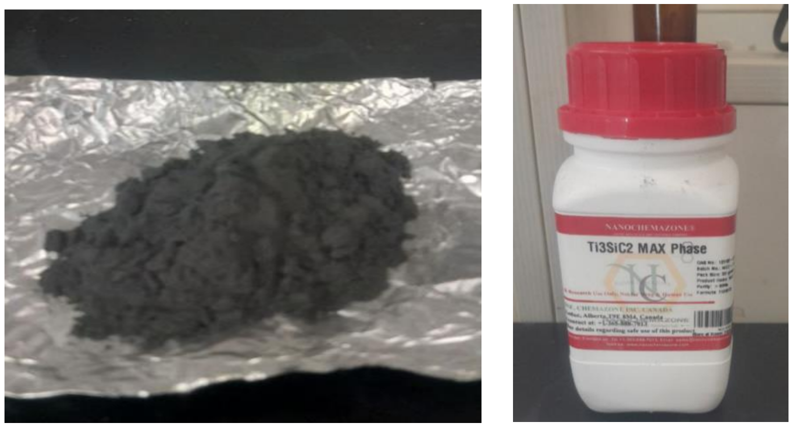

Figure 3.2 Titanium Silicon Carbide (Ti_3SiC_2)

3.1.2.2. Molybdenum Disulfide (MoS_2)

Molybdenum disulfide is an inorganic compound with a chemical formula of MoS_2, composed of molybdenum and sulfur and it is used as a dry lubricant. Table 3.6, 3.7 and Figure 3.3 illustrate the properties, composition and image of MoS_2 used respectively.

Table 3.6 Molybdenum disulfide

Physical and mechanical Properties	Molybdenum disulfide
Color	Lead Gray to Black
Density g/cm^3	5.06
Crystal structure	Hexagonal-Layered
Coefficient of friction	0.03-0.06
Molecular weight (gr/mol)	160.06
Melting point (℃)	1185
Thermal conductivity at 300 K (W/cm-K)	0.014
Hardness (Mohs Scale) basal plane	1-1.5

Table 3.7 Chemical composition of MoS_2

Chemical (wt. %)	molybdenum disulfide (MoS_2)
Fe	0.04 (1)
Ni	0.07 (2)
Cu	0.08 (2)
Sn	0.01 (1)
Au	0.05 (2)
Re	0.02 (1)
Mo	59.83 (40)
S	39.96 (29)
Se	0.01 (1)
Total	100.07 (42)

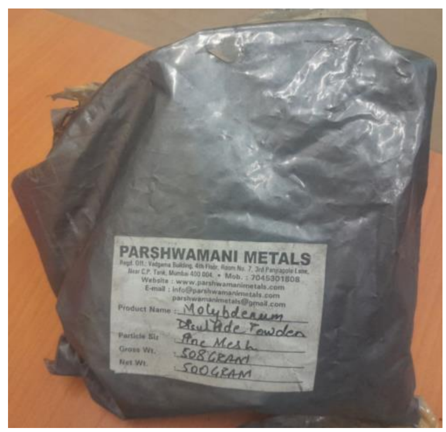

Figure 3.3 Molybdenum Disulfide

3.1.2.3. Graphene oxide (GO)

Graphene oxide (GO) is a carbon-based layered structure characterized by the presence of oxygen-containing functional groups (=O, -OH, -O-, -COOH) on both sides of the layers and along the edges of the plane. Properties, composition and images of GO are shown in Table 3.8, 3.9 and Figure 3.4 below.

Table 3.8 Properties of Graphene Oxide

Physical and Mechanical property	Metric	Unit
Density	3.6	g/cm3
Tensile Strength	130	MP
Elastic Modulus	230-420	MP
Elongation at Break	0.60	%
Thermal conductivity	0.5-18	$Wm^{-1} K^{-1}$
Electrical conductivity (Sm^{-1})	5.7*10-6	Sm-1

Table 3.9 Composition of Graphene oxide(GO)

Element	Carbon	O	N	H
Content (wt.%)	44.01	52.97	0.2	2.52

Figure 3.4 Graphene oxide

3.1.3. Equipment's Used to Fabricate and Prepare Composite Sample

Table 3.10 presents the equipment utilized for the fabrication of the hybrid Copper matrix composite, as well as the equipment employed for the preparation of experimental samples.

Table 3.10 Fabrication and Sample preparation equipment's

Equipment's	Task	Model
Furnace	To melt the copper alloy	Electrical Furnace
Stirrer	To uniformly distribute the reinforcement(s) throughout the matrix metal	Fabricated locally form stainless steel
Sand paper /Polisher	To obtain a flat and smooth surface free from excessive deformation.	P220, P400, P800, P1200, P2000
Hand drill	To give uniform distribution by providing rotational motion to stirrer after the stirrer is attached to hand drill	
Lathe machine	To prepare specimen for tribological and mechanical tests	Pinocho, SP/250
Abrasive Cutter	Abrasive cutter is used method for sectioning materials during sample preparation for testing.	RB 203 Abcut-M
Chemical etchant	To prepare specimen for micro structural characterization	Keller's etchant

3.1.3.1. Furnace

It is a tool for melting and heating metals, alloys, and ores in preparation for additional processing. Furnaces have the ability to reach high temperatures and can run on fuel or electricity. When creating the Copper alloy, the alloy is melted in a furnace, usually at a temperature of 1100oC, within a crucible. Furnaces are often constructed using a number of parts, such as a plate-and-angle body frame, blankets, refractory bricks, crucibles, thermocouples, heating coils, temperature controllers, voltage meters, ammeters, and other equipment.

3.1.3.2. Stirrer and hand drill

Mechanical stirring is used in the stir casting process to distribute reinforcements uniformly throughout the matrix material. A stirrer made of a stirrer rod and stirrer blades is required to generate a vortex in the crucible. The stirrer is usually fastened to an electric motor. But in this work, as Figure 3.5 shows, the stirrer was extracted by hand using a drilling tool. The hand drill's parameters are used to establish the stirrer rod's diameter. In this mechanical stirring arrangement, rotational motion is produced by the hand drill, which causes the attached stirrer to form a vortex.

3.1.3.3. Sandpaper/Polisher

Sandpaper, which is sometimes referred to as glasspaper or coated abrasive, is a material that comprises sheets of paper or cloth with an abrasive substance adhered to one side.

3.1.3.4. Lathe Machine

Lathe machines are essential tools in manufacturing, used to perform various operations such as cutting, turning and drillingto shape work pieces into desired forms (Patel GC et al., 2020). These machines can be operated manually or with computer numeric control (CNC) to achieve high precision and efficiency in production (Jha et al., 2021).

Figure 3.5 Lathe machine

3.1.3.5. Chemical Etchant

The microstructural distribution of the reinforcements in the composite specimens was examined and analyzed using an optical microscope both before and after the corrosion test. To provide a clear view, the polished specimens were etched using Keller's etchant, which consisted of 25 milliliters of distilled water, 25 milliliters of $NH4(OH)2$, and 5 milliliters of 30% strength HCl.

3.1.3.6. Abrasive cutter

Abrasive cutter is used to cut bulk samples and produce thin slices of samples as one of sample preparation equipment's for microscopic observation. The Abcut-M is possible cutting form soft materials to hard materials.

3.1.4. Testing Equipment's

The primary apparatus utilized to evaluate the characteristics of the created hybrid copper alloy metal matrix composite is displayed in Table 3.11.

Table 3.11 Testing equipment's

Equipment's	Test name	Model
Analytical Precision Balance	To measure mass of materials	HR-250AZ and AUW320
Universal test machine (UTM)	Compression strength	WP 310 HYDROLIC UTM-Gunt Hamburg
Vickers hardness tester	Hardness test	HVS-50
Optical Microscopy	Microstructure test	Huvitz HR-300 Series
Scanning electron microscope	Wear mechanism examination	JEOL
Micro Pin-on-disk Tribometer	Wear and friction test	TR-20-MICRO
XRD	Phase composition	XRD-7000
Potentiostat	Corrosion test	SP-300 Potentiostat
FTIR spectroscopy	Chemical composition test	is50 ABX

3.1.4.1. Analytical Precision Balance

Digital balances are tools that are used to quantify an object's mass precisely. The mass of the composite for real density measurement, the mass of the composite before and after wear for tribological property analysis, and the mass of the reinforcement(s) and metal matrix in accordance with specifications were all measured in this work using an analytical precision balance. HR-250AZ was utilized for the first two, and AUW320 for the third.

3.1.4.2. Universal testing Machine (UTM)

Compressive strength, tensile strength, and other properties of materials are tested using a universal testing machine (UTM), also known as materials testing machine or a universal tester. Tensometer was the previous name for the tensile testing apparatus. The term "universal" refers to the machine's ability to execute various standard tests on various parts, materials, and structures, including tensile, peel, bending, and compression tests.

3.1.4.3. Hardness testing machine

The Vickers hardness test applies a specified force, F, to a pyramid diamond indenter with a square base and an angle of 136 degrees between the opposing faces at the test piece's surface (B. Wang et al., 2020).

$$HV = \text{Constant X Test force/ surface are of indentation} = 0.102 \text{ x } 2F\,(\sin(136^{o}/2))/d^2$$

Hardness is often understood to be a material's resistance to long-term deformation caused by things like wear, scratches, indentation, abrasion, distortion, etc. Macro- and micro-hardness tests are the two different forms of hardness testing. Stresses delivered to the indenter surpass one kilogram in the micro-hardness test, but loads applied in the macro-hardness test are less than or equal to one kilogram. The materials being tested for microhardness are very thin. A 10 mm diameter hardened steel or carbide ball is used in the Brinell hardness test; a diamond cone or hardened steel ball indenter is used in the Rockwell hardness test; and a diamond indenter shaped like a right pyramid with a square base and an angle of 136 degrees between opposing faces is used in the Vickers hardness test. These are the three available kinds of macro-hardness testing (loads > 1 kg). Additionally, tests for microhardness (load less than 1 kg) such as the Vickers diamond pyramid and the Knop diamond are accessible.

3.1.4.4. Optical microscope (OM)

The optical microscope, sometimes referred to as the "light optical microscope," is a type of microscope that uses lenses and visible light to magnify pictures of tiny materials. The optical variety is the oldest type of microscope and is said to have originated in the seventeenth century in its current compound form. While many advanced versions are made to improve sample contrast and resolution, there are also many of basic optical microscopes accessible. Historically, optical microscopes have been extensively used and easily designed because they use visible light, which permits direct visual viewing of samples (Grieseler et al., 2017).

3.1.4.5. Scanning electron microscope (SEM)

The SEM is a versatile and widely adopted instrument for examining the microstructure of materials by scanning their surfaces. Its applications extend across various fields, from biological research to materials science and engineering, demonstrating its multifaceted utility in scientific investigations (Beb et al., 2022; Shi & Butenko, 2018).

3.1.4.6. Pin on Disk Test

Wear and friction tests, which involve evaluating wear rate and wear resistance of materials, are typically conducted using various types of tribometer. Among these, the pin-on-disk test is widely employed as a common method for characterizing wear and friction properties. This test is popular due to its availability of tribological contacts and simplicity.

The wear and friction experiments are carried out using a pin-on-disk apparatus is accordance with the ASTM G99 standard.

3.1.4.7. FTIR Spectroscopy

Fourier Transform Infrared Spectroscopy (FTIR), also refer to as FTIR Spectroscopy or FTIR Analysis, is an analytical method employed for the identification of infrared light to scan test samples and examine their chemical characteristics. Figure 3.14D provides a schematic representation of FTIR Spectroscopy.

3.2. Methodology

3.2.1. Matrix and Reinforcements composition Selection

Prior to beginning the manufacturing process, it is essential to determine the weight % of reinforcements for each sample in the composite material production process. The weight percentage composition of reinforcements in this study is derived from the literature, and each sample's weight percentage composition is determined by taking into account the following five factors.

- ✓ The mechanical, electrical, and tribological properties of developed samples have mainly relies on the weight percentage (wt%) of reinforcements used. As a result, the weight percentage of Ti_3SiC_2, MoS_2 and GO used in the presented work have been maintained to enhance the mechanical properties of the metal matrix without much affecting its electrical properties.
- ✓ The total wt.% composition of reinforcements should not have to exceed 30% in order to reduce amount of porosity and to prevent aggregation of reinforcements (Arunachalam et al., 2019). Therefore, the maximum amount of reinforcement wt.% included in the composite is 5% not to affect the electrical properties of copper composite fabricated.
- ✓ For electronic applications incorporation of MAX Phase up to 3% on Copper metal matrix is recommended by (Grieseler et al., 2017) and others.
- ✓ To have best tribological impact on the composite, 1:1 GO-MoS_2 is suggested by (Ismail et al., 2021).
- ✓ (Nautiyal et al., 2019) studied the effect of 2wt% GO-MoS2 on Copper at 650, 700 and 750℃ and resulted a remarkable reduction in both the wear rate and the coefficient of friction.

Based on the above consideration, double reinforced (Cu15000 + Ti_3SiC_2 + MoS_2 and Cu15000 + Ti_3SiC_2 + GO), and triple reinforced (Cu15000 + Ti_3SiC_2 + GO + MoS_2) composite materials are fabricated using stir casting methods, and the detailed weight compositions are presented in below under Table 3.12.

Table 3.12 Weight composition of Reinforcements

No	Copper alloy%	Ti_3SiC_2%	GO%	MoS_2%
Double Reinforced				
1	98	1	0	1
2	98	1	1	0
Triple Reinforced				
3	97	1	1	1
4	96	2	1	1
5	95	3	1	1

3.2.2. Estimating Mass of Matrix and Reinforcements Required for Each Specimen

The total weight amount used to fabricate metal matrix composite were calculated to produce optimum sample size for density and porosity test, Wear test, hardness test, FTIR test, corrosion test, SEM and XRD characterization.

The mold used to shape the fabricated copper composite using stir casting has frustum conical shape. It has base diameter of 35mm, top diameter of 65mm and height of 75mm.

$$V = \frac{\Pi h}{3} \frac{(R^3 - r^3)}{3} \quad \text{Eq. (3.1)}$$

Where V = volume of specimen in cm^3

h = height in cm, h = 75mm = 7.5cm

R = Top radius in cm, 65mm = 6.5cm

r = Bottom radius in cm, 35mm = 3.5cm

$$V = \frac{3.14*7.5\text{cm}}{3} \frac{(6.5cm^3 - 3.5cm^3)}{3}$$

$V = 0.6064cm^3$

The density of copper matrix and the reinforcements (Ti_3SiC_2, GO and MoS_2) are:

- ✓ Density of Copper alloy (Cu15000), $\rho_{Cu15000}$ = 8.89 gr/cm^3
- ✓ Density of Silicon carbide (Ti_3SiC_2), $\rho_{Ti3SiC2}$ = 4.5 gr/cm^3
- ✓ Density of Boron carbide (GO), ρ_{GO} = 3.6 gr/cm^3
- ✓ Density of Molybdenum disulfide (MoS_2), ρ_{MoS2} = 5.06 gr/cm^3

The following estimates are made in each specimen for the specified compositions of matrix (Cu15000) and the reinforcements (Ti_3SiC_2, GO and MoS_2).

$$m_x = V_{total} * \rho_n * m \quad \text{Eq. (3.2)}$$

where, n = matrix/ reinforcement

m = weight% of matrix/reinforcement

- ✓ Total weight of copper alloy (Cu15000), $m_{Cu15000}$ = 2652.8 gr
- ✓ Total weight of Titanium Silicon carbide (Ti_3SiC_2), $m_{Ti3SiC2}$ = 43.76 gr
- ✓ Total weight of Graphene oxide (GO), m_{GO} = 21.95 gr
- ✓ Total weight of Molybdenum disulfide (MoS_2), m_{MoS2} = 21.89 gr

3.2.3. Copper Metal Matrix Composite Fabrication

In the fabrication of copper metal matrix composite for this research work, liquid metallurgy specifically stir casting method is used. The process parameter selected and procedures used to fabricate the composite is presented in the preceding sections.

3.2.3.1. Stir Casting parameter selection

To attain the desired properties of metal matrix composites, it is crucial to ensure a uniform distribution of the reinforcement material within the matrix alloy. Additionally, it is important to optimize the wettability or bonding between these components while minimizing porosity levels.

For this research stir casting is used based on its most economical way of fabricating copper and application of high temperature on the metal matrix in addition to stirring process gives uniform distribution of reinforcement(s).

The parameters used to fabricate the copper composite using stir casting liquid metallurgy process is selected based on different literature survey, some of these are mentioned below.

- ✓ (Vairamuthu et al., 2021) Investigated the optimum stirring time to uniformly distribute the pre heated reinforcement in the copper metal matrix and also it is helpful in removing unwanted particles form the molten metal. For this 30, 40, and 50 min was used and applying of 40 min stirring time was noted to be optimum to enhance the tensile strength, hardness, and impact strength of the composite fabricated.
- ✓ Research on the rotational speed of stirrer was developed using different rotational speed on the same composition of Cu-Al alloy. The effect of stirring speed on the effect of Micro-hardness, Toughness and UTS was analyzed using grey relational analysis. Accordingly, from 410, 420, 430, 440 and 450 rpm the best result was attained while using 430rpm (Das et al., 2016).

- ✓ Different researchers have been using stir casting temperature of 1100°C for manufacturing of copper metal matrix composite depending on the melting point of Cu (Mohan et al., 2023; Vairamuthu et al., 2021) and others.
- ✓ The preheating temperature for hybrid metal matrix composite was effectively utilized at 550°C, shortly before pouring the reinforcements in to the metal matrix (Dmitruk & Naplocha, 2022).

Based on the above mentioned and other reviews, the stir casting parameters for the fabrication of Copper metal matrix composite in this paper is used as for sown in table 3.13 below.

Table 3.13 Operating Conditions for stir casting process

Operating Conditions for stir casting process	Metric	Unit
Stirring Speed	430	rpm
Stirring Time	40	min
Pouring Temperature	1100	°C
Preheating Temperature	550	°C

The electrical stir casting used for this research needs 250-300°C calibration, so fully melted metal matrix is obtained at around 800°C based on the controller reading.

3.2.3.2. Stir Casting Procedures

The productions of copper alloy metal matrix composite reinforced with T_3SiC_2, GO, and MoS_2 was carried out using liquid metallurgy specifically the stir casting method. Due to its simplicity, the stir casting process is widely used in the production of composite materials. Using this technique, reinforcements are mechanically agitated into a molten metal matrix. Following that, the liquid composite material may be cast using standard casting methods and subsequently processed using normal metal forming processes like extrusion, forging, and others (Arunachalam et al., 2019).

(a) (b)

Figure 3.6 Stir casting set up A) Electrical furnace and B) Controller

Steps involved in the fabrication of copper metal matrix are: -

- ✓ Measure the mass of copper matrix and reinforcements according to the specified ratios in Table 3.12 for each specimen.
- ✓ Place the Copper alloy into a graphite crucible and turn on the electrical furnace inside to initiate the melting process. Allow the furnace to run for a few minutes to ensure that the specified temperature (1100 ^{o}C) is attained and Copper alloy reaches a fully molten state.
- ✓ To enhance wettability and eliminate moisture content, preheat the reinforcements, promoting improved bonding with the matrix material.
- ✓ Next, the preheated reinforcements were introduced into the molten copper alloy in two stages and mechanically stirred at a rotational speed of 550 rpm for duration of 40 minutes, ensuring the even dispersion of the reinforcements throughout the mixture.
- ✓ Following the stirring process, any slag present in the molten Copper mixture was eliminated. Subsequently, the molten mixture was poured into a prepared sand mold, allowing it to solidify within the mold cavity.
- ✓ Subsequently, the composite was extracted from the mold once it had solidified, following the procedure illustrated in Figure 3.6. The produced specimens were fabricated in accordance with ASTM standards, enabling them to undergo various tests as required.

3.2.4. Specimen preparation for testing and characterization

Following the successful fabrication of the composite material through the stir casting method, the composite was prepared for a series of tests, including , physical testing, mechanical testing, microstructural characterization, and tribological testing. To meet the requirements of ASTM standards, the specimens were machined to the specified shape and size using a lathe.

3.2.4.1. Machining and cutting

To address the issue of rough surfaces and undesired features on the fabricated composite, machining on a lathe and milling was performed as shown in Figure 3.7. This machining process aimed to reduce surface roughness, eliminate unwanted parts, and achieve the desired shape and size in accordance with the specifications outlined by ASTM standards.

(a) (b)

Figure 3.7 Machining of casted sample on a (a) lathe machine and (b) milling machine.

3.2.4.2. Grinding, Polishing and Etching of specimens

The primary purpose of grinding and polishing specimens is to create a flat surface, eliminate cut marks, and achieve a level surface that is free from excessive deformation. This process involves several steps, including rough grinding, fine grinding, and polishing.

In the initial step, cut specimens are subjected to grinding using sandpaper of various grit sizes, including 120, 240, 400, 800, 1200, and 2000 grits. This grinding process aims to eliminate any surface imperfections and artifacts, resulting in a smoother surface. To achieve a mirror-like finish, polishing is then carried out using diamond suspension, as depicted in Figure 3.9B During this process, it is important to apply moderate pressure initially and gradually reduce it to prevent plastic deformation of the specimen. A two-wheel system, specifically the RB 204 Metpol-II

Model polishing machine with motor control capable of operating at speeds ranging from 50 to 500 rpm, was utilized for this purpose.

Additionally, etching using Keller's chemical etchant was performed. Etching involves selective chemical attack to reveal the microstructural features, such as grains and grain boundaries, more clearly. Keller's chemical etchant is recommended for Copper and Copper alloys. Accordingly, the amount of chemical etchant added in the fabricated copper matrix composite is shown in Table 3.14. Additionally Figure 3.8C illustrates the etching process carried out on the hybrid composite.

Table 3.14 Etchant used

Etchant	Concentration	Condition
Distilled water	25 ml	
Ammonium hydroxide	25 ml	30 min
Hydrogen peroxide (30%)	5 ml	

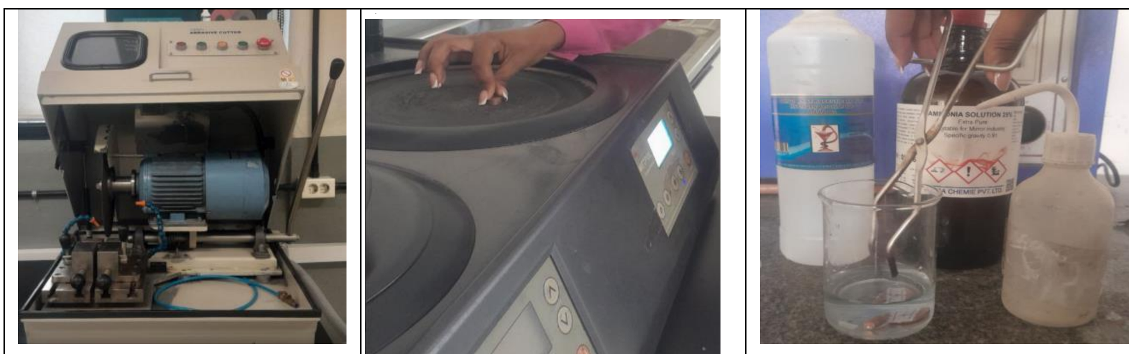

(A) (B) (C)

Figure 3.8 A. Grinding B. Polishing C. Etching

3.2.5. Experimental Analysis

In order to undertake the study, a variety of mechanical and physical parameters, including hardness and compression strength, as well as density and porosity, were investigated experimentally. Tribological characteristics, such as wear loss, corrosion rate, and coefficient of friction, as well as microstructural characteristics, were also investigated. During the course of the experiment, the most important findings from every test were gathered, examined, and shared. In the end, important deductions were made in light of the examined data. The following experiments were carried out in this paper, and a detailed discussion of each experiment's methodology is provided below.

3.2.5.1. Density and porosity measurement

Two physical characteristics of materials are density and porosity. The mass divided by the unit volume is the theoretical definition of a material's density. The weight percentage and density of each laminated hybrid component were used to compute the theoretical composite densities (ρ) using Eq. (3.3) in accordance with the ASTM standard test. Using a digital caliper, the volume of each of the five samples was precisely measured, and the average volume was noted (Salman & Leman, 2018). The experimental densities of the composites were measured by suspending the fabricated composite inside distilled water as shown in figure 3.9 and calculated by dividing their weight by their volume, expressed in grams per cubic centimeter. The fiber volume fraction is the percentage of fiber content in the entire volume of a laminated hybrid composite. It plays a crucial role in determining the overall mechanical response and properties of the composite. Higher fiber volume fractions are generally associated with improved mechanical properties of the composites.

$$\rho_{\text{theoretical}}(\text{g/cm}^3) = \frac{1}{\left(\frac{Wt\%_A}{\rho_A}+\frac{Wt\%_B}{\rho_B}+\frac{Wt\%_C}{\rho_C}+\frac{Wt\%_D}{\rho_D}\right)} \qquad \text{Eq. (3.3)}$$

where, $wt\%_A$, $wt\%_B$, $wt\%_C$, and $wt\%_D$ are the weight percentage of Cu15000, Ti_3SiC_2, GO, and MoS_2 respectively, while ρ_A, ρ_B, ρ_C, and ρ_D densities of Cu15000, Ti_3SiC_2, GO, and MoS_2.

In the experiment, we can formulate the Density hybrid aluminum matrix composite as follows: we calculated the actual density of the composite using Archimedes principle. First, we weighed the cylindrical specimen in air (m_{air}) and then in distilled water (m_{water}). The actual/experimental density (ρ_{actual}) was then calculated using Eq. (3.4) **(Mclinden, 2014).**

$$\rho_{actual}(\text{g/cm}^3) = \frac{mair}{mair-mwater}\,\rho_{water} \qquad \text{Eq. (3.4)}$$

Where: ρ_{actual}= actual/experimental density; m_{air}= mass of composite in air and m_{water} = mass of water in distilled water and ρ_{water} = density of distilled water at 25°C = 997.044 kg/m^3.

The porosity of each hybrid composite material can be assessed using equation Eq. (3.5) (Aatthisugan et al., 2017).

$$P = 1- (\rho actual/\rho theorethical) \quad \text{Eq. (3.5)}$$

Where P = the porosity of composite material, ρ_{actual} = the actual density of composite material and $\rho_{theorethical}$ = the theoretic density of composite material.

Figure 3.9 Experimental density measurements in distilled water.

3.2.5.2. Hardness Test

In this study, the hardness value of a hybrid Copper alloy (Cu15000) matrix composite, which was fabricated using the stir casting technique, was measured using a Vickers hardness tester machine. The hardness tests were conducted on the copper alloy (Cu15000) hybrid composites with varying weight percentages of reinforcement particles. Before the material's hardness was tested, its surface was polished and ground. Ten seconds were given to the test with a weight of 10 kgf applied. The specimens used in the hardness test are 20 mm in diameter and 3 mm in height, as shown in Figure 3.11b.

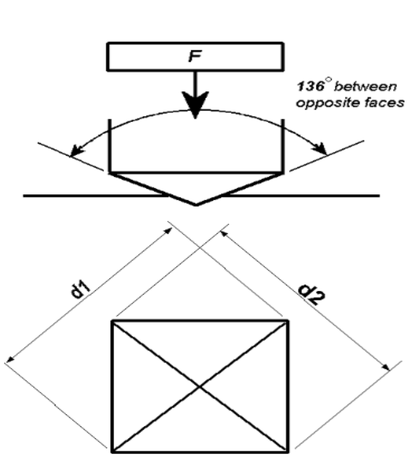

$$HV = \frac{2F\sin\frac{136^2}{2}}{d^2} - 1.854\frac{F}{d^2} \quad \text{Eq. (3.6)}$$

Where F = load in kgf

D = mean of two diagonals, d1 and d2 in mm

HV = Vickers hardness

Figure 3.10 Hardness and Microstructural test specimen 20 mm diameters with 3mm height

(a) (b)

Figure 3.11 Vickers hardness testing (a) machine set up (b) specimen

3.2.5.3. Compression Test

The ultimate tensile strength of a material is defined as the magnitude of uniaxial compressive stress at which the material completely fails. Compressive strength is typically measured through a compressive test, where a uniaxial compressive load is applied to a cylindrical specimen. The specimen was prepared according to the ASTM E-9 standard, with a length-to-diameter ratio of 1.92 (25mm length and 13mm diameter), and tested using a universal testing machine (UTM) shown in Figure 3.12 with a 100KN load capability. The load was applied until the specimens fractured.

Figure 3.12 Universal testing machine (UTM) setup for compression test

3.2.5.4. Wear and Friction test

The progressive loss of mass from a solid body's surface as a result of mechanical forces is referred to as "wear" (Mang et al., 2011). Using a computerized TR-20-MICRO model micro pin-on-disc tribometer and the ASTM G99 standard, room temperature dry sliding wear tests were carried out for this investigation. The components of the tiny pin-on-disc Tribometer equipment are as follows: a disk, a load, a pin holder, and a pin (specimen), as illustrated in Figure 3.13. EN-31 hardened steel was the disk material employed in this experiment. 10N loads were applied while testing the specimen. The test parameters included a constant wear track diameter (50mm), test duration of 10 minutes, and a rotation speed of the disk at 300rpm.

The mass or weight loss of each sample was used to calculate the wear rate (W.R). The wear rate (W.R) of the specimen can be calculated using Eq (3.5) through the weight technique. This method provides a more accurate result for wear compared to other weight techniques (Gonfa et al., 2022).

$$W.R = \frac{wear\ volume\ loss}{sliding\ distance} = \frac{V_L}{\Pi dnt} = \frac{W_L}{\rho \Pi dnt} \quad \text{Eq. (3.7)}$$

Where, W.R is wear rate, d is the diameter of the wear track of the disc (50mm), n is revolution per minute (300rpm), t is time (10 minutes), and W_L is the weight (or mass) loss (Weight before wear (W_b) – weight after wear (W_a)).

As per the ASTM G-99 standard, a composite specimen was made in order to evaluate the tribological characteristics. A specimen holder held the 5.9 mm in diameter and 12 mm in height, which was then forced up against a revolving disk while certain computer-controlled parameters were in place. Wear loss and the coefficient of friction were continually monitored and recorded during the test. The wear test device's inbuilt computer provided the coefficient of friction against time graph. A precision balance that was calibrated to an accuracy of ± 0.0001g was used to calculate the wear loss. The pin-on-disk wear testing apparatus is shown in the following picture 3.13.

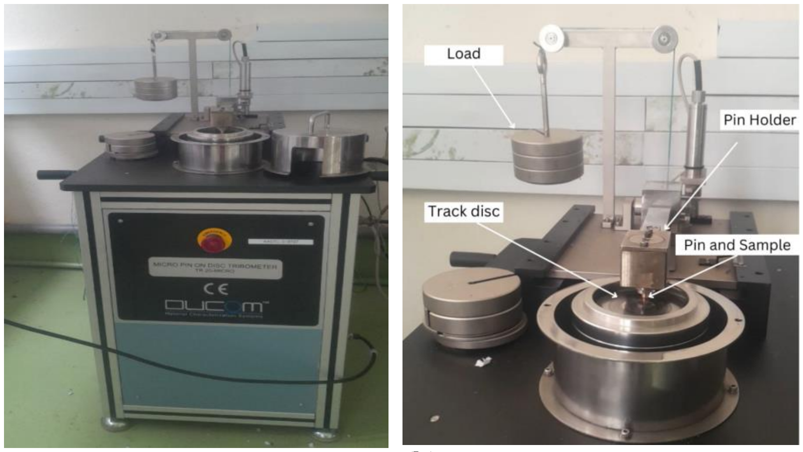

(a) (b)

Figure 3.13 Pin on disk

3.2.5.5. Microstructural Analysis

To investigate different behavior of a material characterization is very important. In this research work four characterization techniques are used. Optical microscope is used to study the porosity and grain boundaries of samples prepared, SEM is also used to see uniform distribution of reinforcement in the metal matrix and to study wear morphology of the optimized samples, XRD is used to see the finger print of the composite, and FTIR is used to study the synergetic effect of the composite using the functional groups.

The following figure shows the equipment's used to perform microstructural characterization of composites fabricated.

(A) (B) (C) (D)

Figure 3.14 A) Optical Microscope B) SEM C) XRD D) FTIR Spectroscopy

3.2.5.6. Corrosion Test

Corrosion tests were conducted using SP-300 potentiostat Biologic instrument shown in Figure 3.15 by inserting the fabricated and machined specimens in a 3.5% NaCl solution for 30 minutes. A specimen with a diameter of 15mm and a length of 3mm. In order to remove any stray markings and achieve a mirror-like polish, the specimens were intially polished with emery 1200 grit polish paper following with 12 m diamond paste using a double disc polishing machine.

For the electrochemical tests, the working electrodes were copper alloy-based composite specimens with an exposed area of 1cm^2. The auxiliary (counter) electrode was made of graphite, while the reference electrode was either a standard calomel electrode (SCE) or a mercury electrode. Tafel curves were obtained by automatically adjusting the electrode potential from -250 to +250 mV with respect to the corrosion potential (Ecorr), at a scan rate of 1 mV/s.

The impact of reinforcing content on the corrosion behavior of composites made by powder metallurgy was examined through experimentation. Electrochemical data, such as the corrosion potential (Ecorr), corrosion current density (Icorr), and corrosion rate (Cr), were supplied via the Tafel polarization curves. The corrosion potential (Ecorr) and corrosion current density (Icorr) were computed using the anodic and cathodic areas of the Tafel plots. The determination of the corrosion potential and corrosion current densities (Icorr) was achieved by extending the linear segments of the anodic and cathodic curves.

Finally, the corrosion rates were calculated using the following equation (Hallem & Dawood, 2018):

$$\text{Corrosion rate}=\frac{0.13icorr(EW)}{\rho} \qquad \text{Eq. (3.8)}$$

Where,

E.W= equivalent weight

ρ= density

0.13= metic and time conversion factor

icorr= Icorr/A =current density(μA/cm^2)

Icorr = Total total corrosion current and

A = exposed specimen area, cm^2 = 1.76625 cm^2

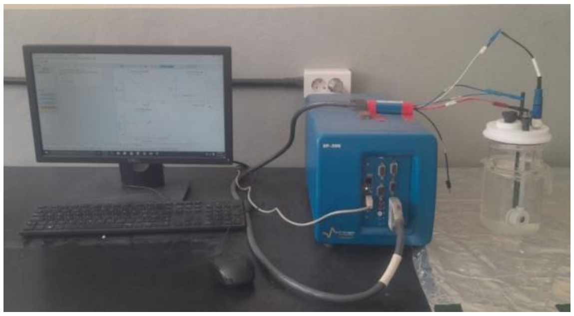

Figure 3.15 Corrosion test Setup

3.2.5.7. Electrical Conductivity Test

An electrical conductivity test was calculated using a digital multimeter. A digital multimeter is an electronic device that is used to measure a variety of electrical properties, such as current, voltage and resistance. The measurements are displayed on a digital screen, which makes it convenient to accurately read and comprehend the results (Ali et al., 2021).

In the research the resistance value obtained from multimeter reading is used to calculate the electrical conductivity of the specimens.

$$\text{Electrical conductivity} = 1/\rho \qquad \text{Eq. (3.9)}$$

Where, ρ= electrical resistivity

$$\rho = RA/l \qquad \text{Eq. (3.10)}$$

where, R= resistance, A= cross sectional area and l= length of specimen

The specimens used for testing had a diameter of 20mm and a length of 3mm. The surface preparation of the specimens remains the same as that of the corrosion test.

3.2.6. Optimization using Taguchi based Grey Relational analysis

3.2.6.1. Grey relational analysis

Prior to normalizing the raw data, grey relational analysis requires preparing the data. Next, the S/N ratio is linearly normalized between 0 and 1. The term "grey relation generation" refers to this process.

Prior to normalizing the raw data, grey relational analysis requires preparing the data. Next, the S/N ratio is linearly normalized between 0 and 1. This process is known as the "grey relation. "By using Grey Relational Analysis (GRA), sixteen subsystems are created from the sixteen experiments. The effect of these subsystems on the response variable is then examined using the GRA approach. We may get lowest values for surface roughness, roundness error, and delamination by ascertaining the parametric criteria linked to the greatest weighted grey relational grade. This enables us to use the creation of the GRA approach to successfully transform the multi-objective problem into a single-objective optimization.

The grey relational coefficient is computed for different process features in grey relational analysis. The grey relational grade is the mean of these coefficients. Next, this grade is utilized in the Taguchi L16 experimental design as a single answer. This procedure is shown in the steps that follow.

Step 1: Transform the original response data into S/N ratio (Y_{ij}) using the appropriate formula depending on the type of quality characteristics using Eq. 3.11, Eq.3.12, Eq.3.13.

Step 2: The performance characteristics are normalized by the selection of an experimental design based on the levels of the process parameters. Yij is normalized as Zij ($0 \leq Zij < 1$) using the following formula in order to minimize variability and prevent the effect of using various units. The original data must be normalized before being subjected to grey relation theory analysis or any other kind of methodology. To get this array's value close to 1, a suitable value is inferred from the values in the same array. We also examined the normalization process's sensitivity to the sequencing outcome, as it has an impact on rank. Therefore, while normalizing data for gray connection analysis, we advise using the S/N ratio value.

S/N ratio with larger the better manner:

$$Z_{ij} = \frac{Y_{ij} - \min(Y_{ij}, i = 1, 2, ...n)}{\max(Y_{ij,}\ i = 1, 2, ...n) - \min(Y_{ij,} i = 1, 2, ...n)}$$ Eq. (3.11)

S/N ratio with smaller -the better manner:

$$Z_{ij} = \frac{\max(Y_{ij}, i = 1, 2, ...n) - Y_{ij}}{\max(Y_{ij,}\ i = 1, 2, ...n) - \min(Y_{ij,} i = 1, 2, ...n)}$$ Eq. (3.12)

S/N ratio with nominal the best:

$$Z_{ij} = \frac{(Y_{ij} - Target) - \min(|y_{ij} - Target|, i = 1, 2, ..., n)}{\max(|Y_{ij} - Target|, i = 1, 2, ..., n) - \min(|y_{ij} - Target|, i = 1, 2, ..., n)}$$ Eq. (3.13)

Step 3: Calculation of the grey relational coefficient and the grey relational grade.

$$\gamma(Y_o(k), Y_i(k)) = \frac{\Delta\min + \xi\Delta\max}{\Delta_{oj}(k) + \xi\Delta\max}$$ Eq. (3.14)

Where, a. j=1, 2…n; k=1, 2…m, n is the number of experimental data items and m is the number of responses.

b. $Y_o(k)$ is the reference sequence ($Y_o(k)$=1, k=1, 2…., m; $Y_j(k)$ is the specific comparison sequence.

c. $\Delta_{oj} = \|Y_o(k) - Y_i(k)\|$ The absolute value of the difference between $Y_o(k)$and $Y_j(k)$.

d. $\Delta\min = \min_{\forall j \in i} \min_{\forall k} \|Y_o(k) - Y_j(k)\|$ is the smallest value of $Y_j(k)$.

e. $\Delta\min = \max_{\forall j \in i} \max_{\forall k} \|Y_o(k) - Y_j(k)\|$ is the largest value of $Y_j(k)$.

f. ζ is the distinguishing coefficient which is defined in the range $0 \le \zeta \le 1$(the value may adjust based on the practical needs of the system).

Step 4: ANOVA for grey relational grade to analyze the experimental results.

$$\bar{\gamma} = \frac{1}{k}\sum_{i=1}^{m}\gamma_{ij}$$

Eq. (3.11)

Where, $\bar{\gamma}$ is the grey relational grade for the j^{th} experiment and k is the number of performance characteristics.

The grade is considered for optimizing the multi-response parameter design problem.

Step 5: Selection of optimal parameters using graph method or ANOVA response table for the grey relational grade.

Better product quality is indicated by a higher gray relationship grade. Because of this, we may use the gray relational grade to evaluate the factor influence and establish the ideal level for every controllable component (Abilash & Sivapragash, 2016).

3.2.7. Flow Chart of This Research Work Methodology

Experimental investigation and optimization of copper metal matrix reinforced composite material has been proposed in this work. The flow chart for the work is presented as follow.

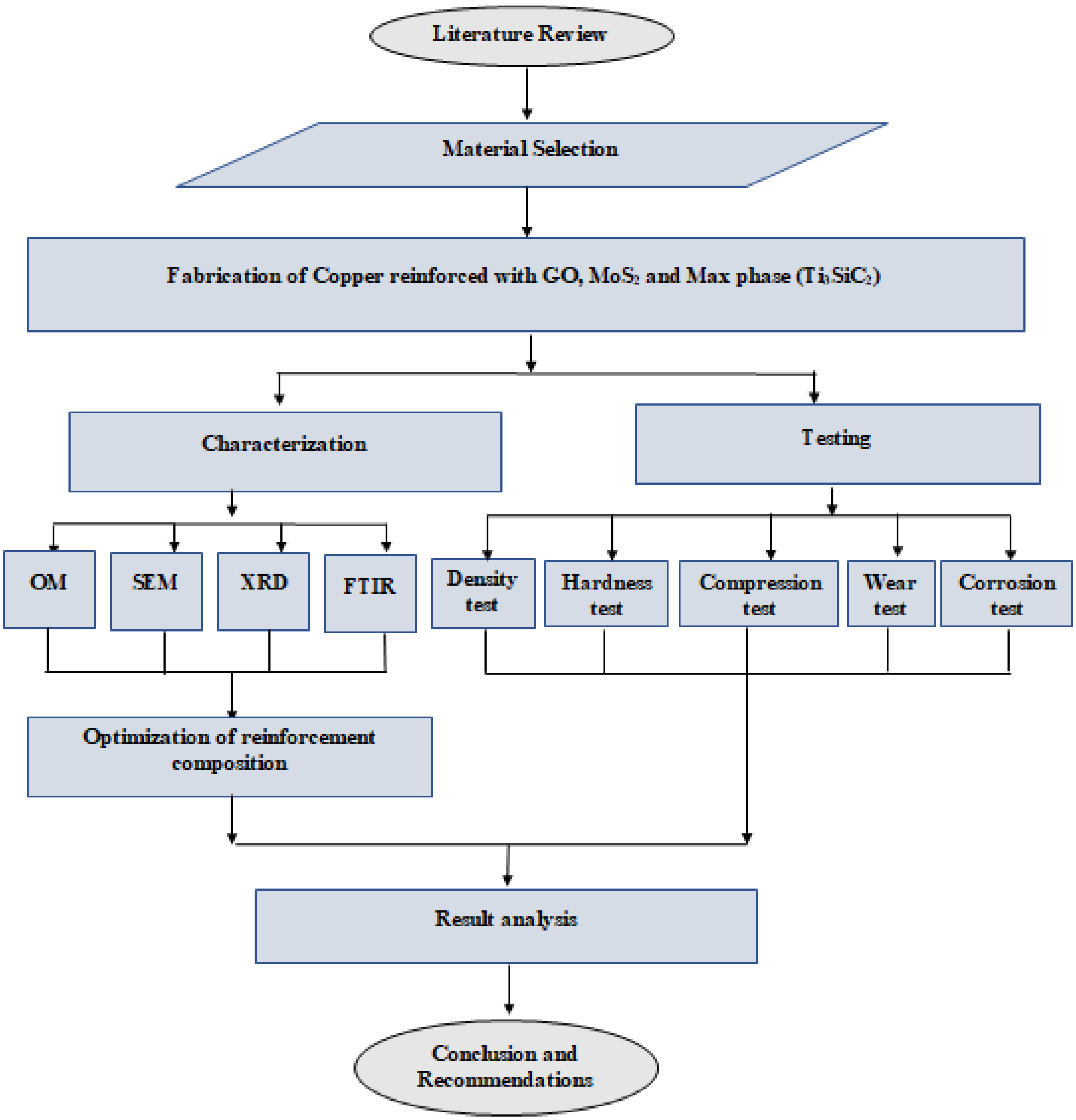

Figure 3.17 Flow chart of overall research work

CHAPTER FOUR

RESULT AND DISCUSSION

4.1. Introduction

The preceding section of the analysis provides a detailed examination of the experimental results conducted in the study. Various sections and subsections are dedicated to discussing the findings in a logical flow. The analysis covers a range of aspects, including density and porosity determination, hardness testing, compression testing, wear testing, corrosion testing, electrical conductivity testing, optimization, material characterization and optimization of tresults for the composite that was fabricated. The results are thoroughly reported and analyzed to offer comprehensive insights.

4.2. Density and Porosity

Density and Porosity are the physical property of the material. In theory, the density of a material is typically defined as the mass divided by the unit volume. The theoretical density of the hybrid composite material developed in this study is calculated using the rule of mixture, as shown in equation (3.4). The actual density, on the other hand, is measured using the rule Archimedes' principle, as shown in Equation (3.5). The determination of the porosity of each hybrid composite material can be achieved through appropriate analysis and measurement techniques using Eq. (3.3).

Figure 4.1 demonstrates the actual and theoretical density of Cu15000 hybrid matrix composites which is also indicated in Table 4.1. As it can clearly show the theoretical density amount is higher for the entire sample measured and this is due to impurities and voids created in the fabrication process.

Table 4.1 Density and Porosity of hybrid Cu15000 matrix composite

Designation	Composite Composition	Theoretical density(g/cm)	Actual density (g/cm)	Porosity (%)
S1	Cu15000 1%Ti_3SiC_2, 1% MoS_2	8.74	8.43	3.55
S2	Cu15000 1% Ti_3SiC_2, 1%GO	8.68	8.52	1.83
S3	Cu15000 1% Ti_3SiC_2, 1%GO, 1% MoS_2	8.61	8.37	2.83
S4	Cu15000 2% Ti_3SiC_2, 1%GO, 1% MoS_2	8.53	8.34	2.26
S5	Cu15000 3% Ti_3SiC_2, 1%GO, 1% MoS_2	8.45	8.27	2.11

As stated in chapter 3, copper alloy (Cu15000) has a density of 8.89g/cm^3, while copper composites have a lower theoretical density compared to the metal matrix. This is because the reinforcement nanoparticles have less dense properties. Therefore, the higher the weight percentage of the reinforcement particles, the less dense the composite becomes.

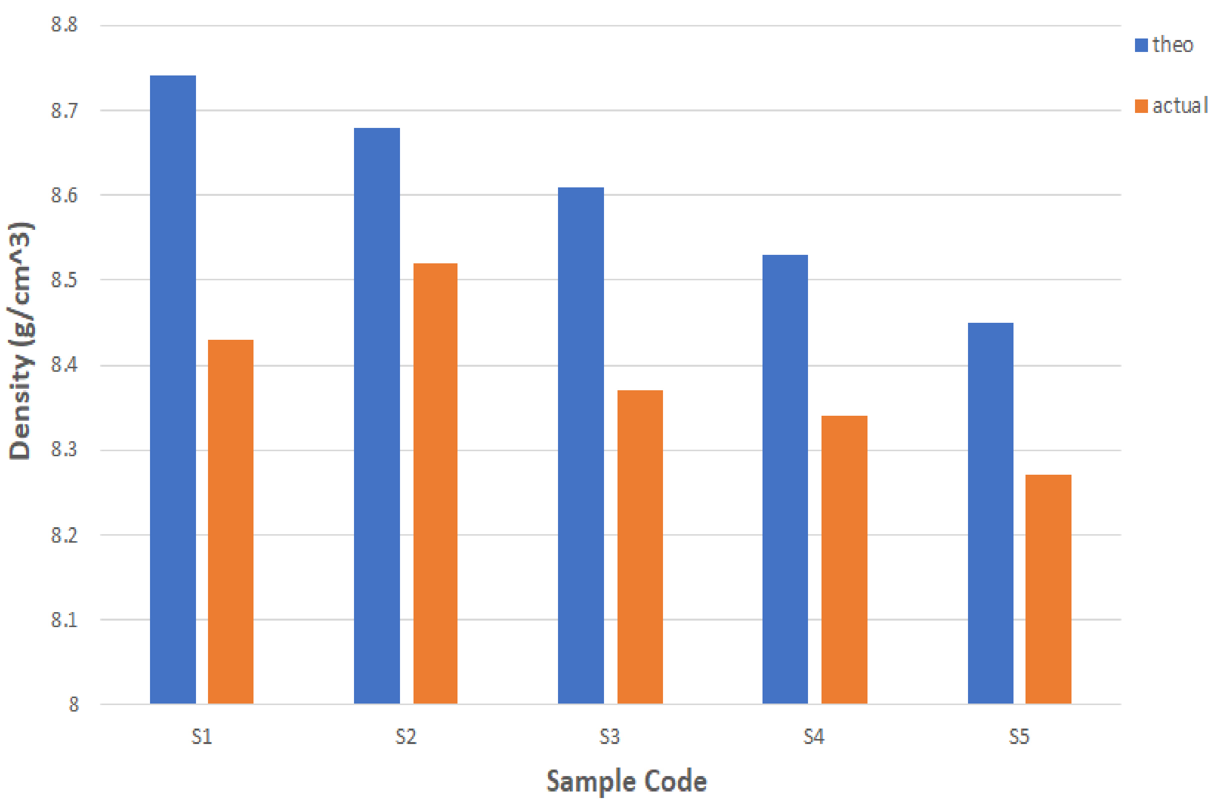

Figure 4.1 Actual and theoretical density of hybrid copper alloy composite

Liquid metallurgy methods, such as stir casting and squeeze casting, are widely employed in the production of metallic composites. However, a common issue arises due to the higher density of copper, causing the reinforcement particles to float above the molten metal. This is because the molten copper does not effectively adhere to the surface of the reinforcement particles, resulting in rejection. Additionally, the casting operation having high temperature above 1100 °C leads to undesired reactions at the interface and chemical breakdown of the particles. As a consequence, segregation of the reinforcement particles and the formation of porosity become more likely to occur (Dinaharan & Albert, 2023). According to (Shankar et al., 2018), porosity levels ranging from 2-4% are considered acceptable in cast composites. Based on Figure 4.2 in Table 4.1, the porosity level of the hybrid composite produced falls within the range of 1.83-3.55%, which aligns with the acceptable levels mentioned in the report. These findings demonstrate the high efficiency of the stir casting technique in manufacturing hybrid copper alloy composites. The addition of MoS_2 and GO has increased the wettability of the metal matrix and reinforcement. Additionally using optimum stirring rotational speed and time helps the reinforcement to distribute evenly and produce less porous metal.

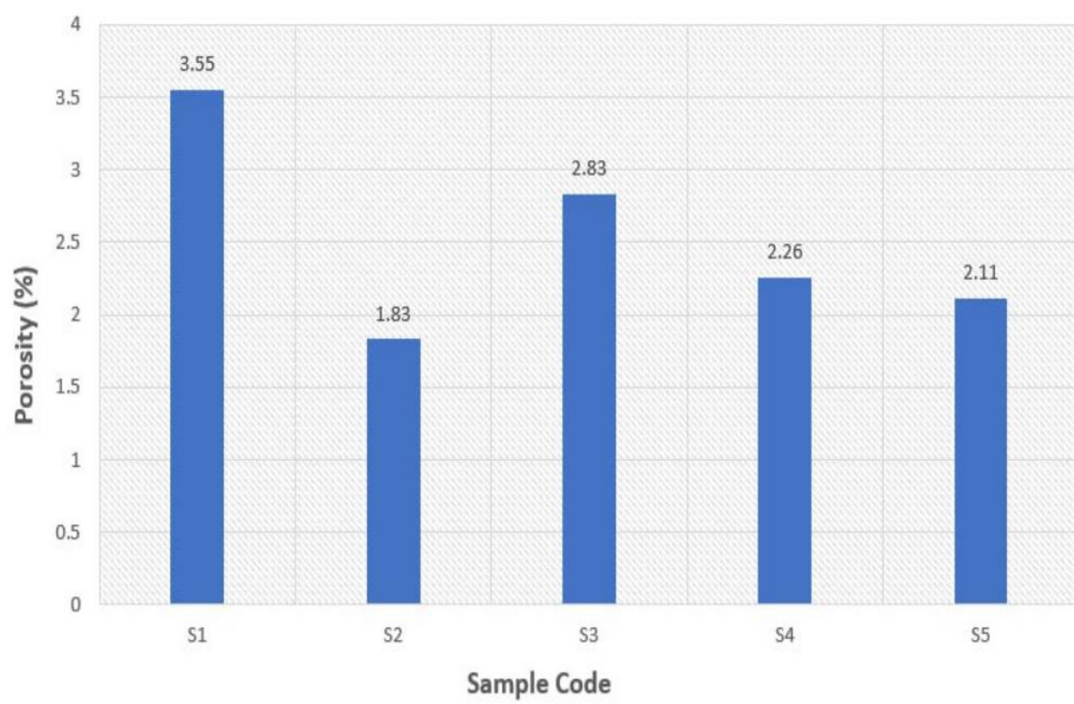

Figure 4.2 Porosity of hybrid copper alloy composite

4.3. Hardness Test

The Vickers hardness measures the overall bonding strength that arises from the individual bonds within a solid material. The hardness of solids provides valuable information about their physical processes, including plastic deformation, depth of indentation, penetration, and scratching (Ali et al., 2021).

A Vickers hardness test was conducted using a Vickers hardness tester machine to determine the scratch and penetration resistance of the hybrid composite. A 10kg.f load was applied for duration of 10 seconds. Table 4.3 displays the results of the Vickers hardness test for each hybrid copper alloy (Cu15000) matrix composite. Three trials were conducted for each composite, and the average value was calculated. Figure 4.7 clearly shows that the hardness of the hybrid composite is higher compared to the cast copper alloy (Cu15000) without any reinforcement.

Table 4.2 Hardness strength of developed hybrid copper alloy composite

No	Vickers Hardness results in HV			Average Vickers Hardness value (HV)
	1	2	3	
1	275.3	193.5	256.2	241.67
2	311.4	299	319.2	309.87
3	296.6	299	361.4	319.00
4	353.5	317.9	369.5	346.97
5	366.2	436.9	334.3	379.13

The hardness measurement results are displayed in Fig. 4.8. The hardness of the copper alloy increases with the addition of reinforcements. The hardness improvement is 87%, 140%, 151%, 169%, and 194% when 1Ti3SiC2-1MoS2, 1Ti3SiC2-1GO, 1Ti3SiC2-1MoS2-1GO, 2Ti3SiC2-1MoS2-1GO, and 3Ti3SiC2-1MoS2-1GO reinforcement is applied respectively, resulting in an increase in hardness from 129 to 379 HV. This increase in hardness can be attributed to the grain refinement observed in Fig. 7. In total, the copper alloy experiences a 194% improvement, which is due to the contribution of an increased percentage of Ti3SiC2 particles.

32.83%, 62% and 129% hardness improvement was observed by the addition of 10wt% of MoS2, 1% Go and 2% rGO-MoS2 reinforcement on pure copper by (Nautiyal et al., 2019; Nazeer et al., 2019; Yehia et al., 2023), However in this research up to 194% hardness increment is observed by reinforcing with Ti3SiC2-MoS2-GO.

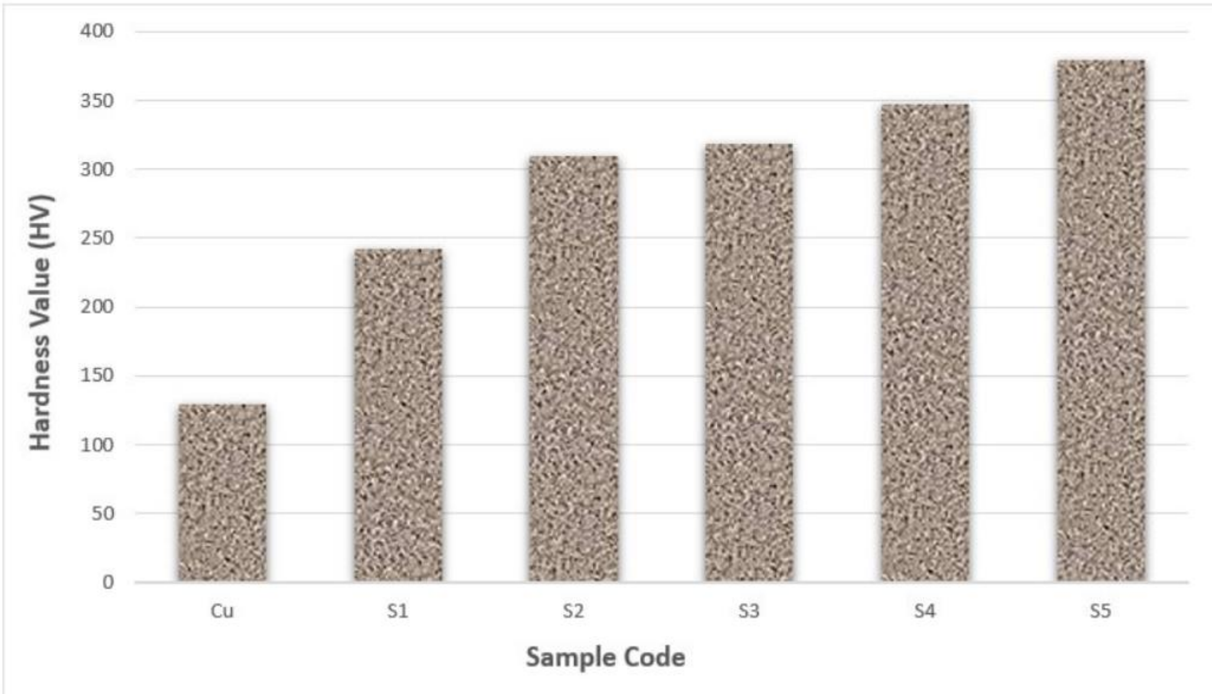

Figure 4.3 Hardness value of hybrid copper alloy composite

The composite fabricated by the application of 3%Ti_3SiC_2/MoS_2/GO achieves the highest level of hardness, showing an improvement of approximately 194% compared to the base metal matrix.

4.4. Compression Test

Casted specimens were subjected to compression testing using universal testing equipment. The results, presented in Figure 4.5 as a bar chart, demonstrate the compression strength of different samples. The ultimate compressive strengths (in MPa) for the copper alloy (Cu15000) samples and those reinforced with Ti_3SiC_2-MoS_2-GO at various weight percentages are as follows: Cu-1500 (295 MPa), Cu-1Ti3SiC2-1MoS2 (397 MPa), Cu-1Ti3SiC2-1GO (365 MPa), Cu-1Ti3SiC2-1MoS2-1GO (473 MPa), Cu-2Ti3SiC2-1MoS2-1GO (524 MPa), and Cu-3Ti3SiC2-1MoS2-1GO (540 MPa).

Table 4.3 Compressive strength of hybrid composite

Composition	Compressive strength (MPa)
Cu-1Ti3SiC2-1MoS2	397
Cu-1Ti3SiC2-1GO	365
Cu-1Ti3SiC2-1MoS2-1GO	473
Cu-2Ti3SiC2-1MoS2-1GO	524
Cu-3Ti3SiC2-1MoS2-1GO	540

The findings indicate that the addition of Ti_3SiC_2-MoS_2-GO reinforcement up to 5% by weight results in higher yield strength compared to the base copper alloy.

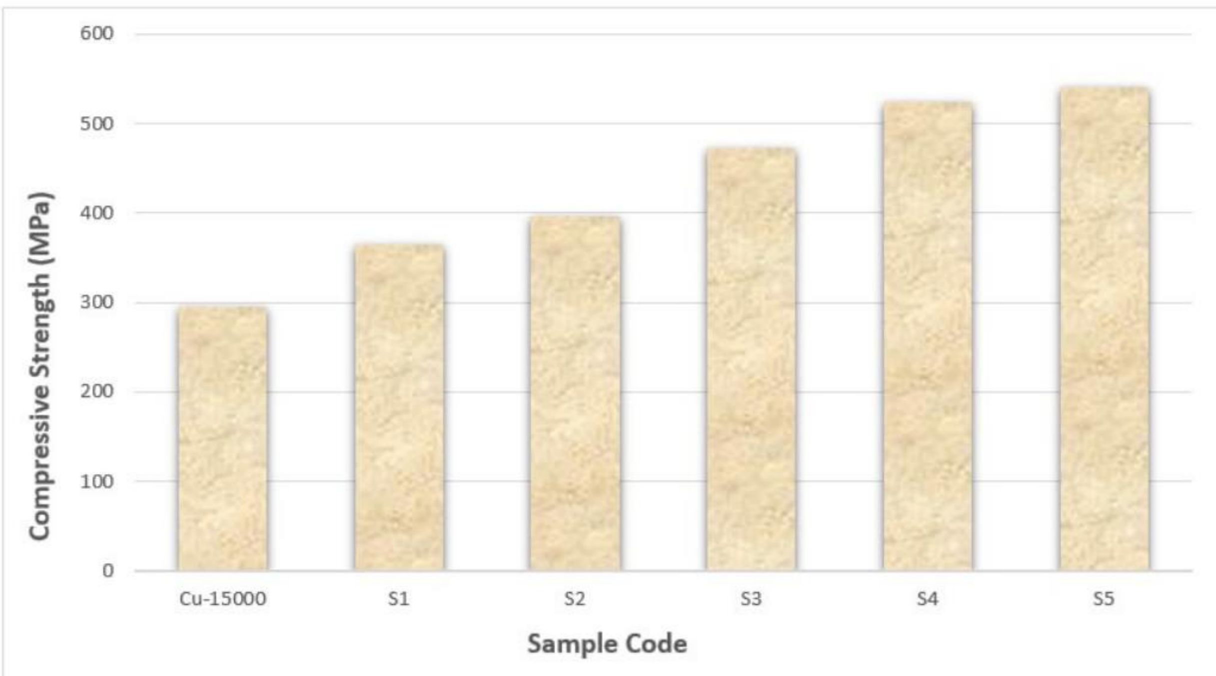

Figure 4.4 Compressive strength of Cu-Ti_3SiC_2-MoS_2-GO Composite

The explanation for the observed results is that as the percentage of reinforcement increased, the quantity of porosity in the microstructure decreased due to higher density of T3iSiC2, thereby positively affecting the mechanical properties. Therefore, since the particles are uniformly and adequately distributed within the matrix, adding them up to a 3% of Ti3SiC2 as observed in this study, has potentially enhance the compressive strength of the composites.

Application of 5wt% rGO increases the flexural strength by 31.3%, compressive strength is approximately 10 time flexural strength, which have direct relationship with each other (Pratik et al., 2020). Based on the investigation of (Su et al., 2022), reinforcing copper-tin alloy with graphite and MoS2 increases the compression strength of the composite by 30%. As it is discovered in this research work, there is up to 83% increment of compressive strength by the application of Ti_3SiC_2-MoS_2-GO reinforcement.

4.5. Wear and Friction Test

The wear loss and coefficient of friction of the hybrid copper composites were measured using a micro pin-on-disc wear tester (TR-20-MICRO) in accordance with the ASTM G-99 standard. The tests were conducted under dry sliding conditions at atmospheric temperature (25^{o}C). The wear tests were carried out at constant loads 30N and a speed of 300 RPM, with a sliding diameter of 50mm. The specimens used had a diameter of 5.9mm and a length of 12mm. The weight of the specimens before and after the wear tests was measured using an analytical balance (SHIMADZU AUW320) with an accuracy of ±0.0001g.

Table 4.4 Mass loss and wear rate of the samples at a specified load

Sample	Reinforcement %	Mass loss (g)	Wear rate (x 10-8 m3/m)
S1	2%	0.0103	0.25
S2	2%	0.0095	0.23
S3	3%	0.0085	0.21
S4	4%	0.0056	0.14
S5	5%	0.0034	0.09

The mass loss (g) and coefficient of friction (COF) were determined in the test. Table 4.4 provides a list of COF values corresponding to different weight compositions. Figure 4.8A illustrates the relationship between COF and time variation.

Table 4.5 Coefficient of friction (COF) for the samples

Sample Code	Coefficient of friction (COF)
S1	0.28
S2	0.45
S3	0.225
S4	0.22
S5	0.165

The coefficient of friction tends to increase over time due to the generation of heat during prolonged sliding. This increase in temperature leads to an elevated coefficient of friction.

According to investigation by (B. Chen et al., 2018; Liu et al., 2019), MoS_2 has a greater reduction effect on the Coefficient of Friction (COF) compared to GO. Similarly, in this research, the application of double reinforcement also shows that MoS_2 has a more significant COF reduction effect.

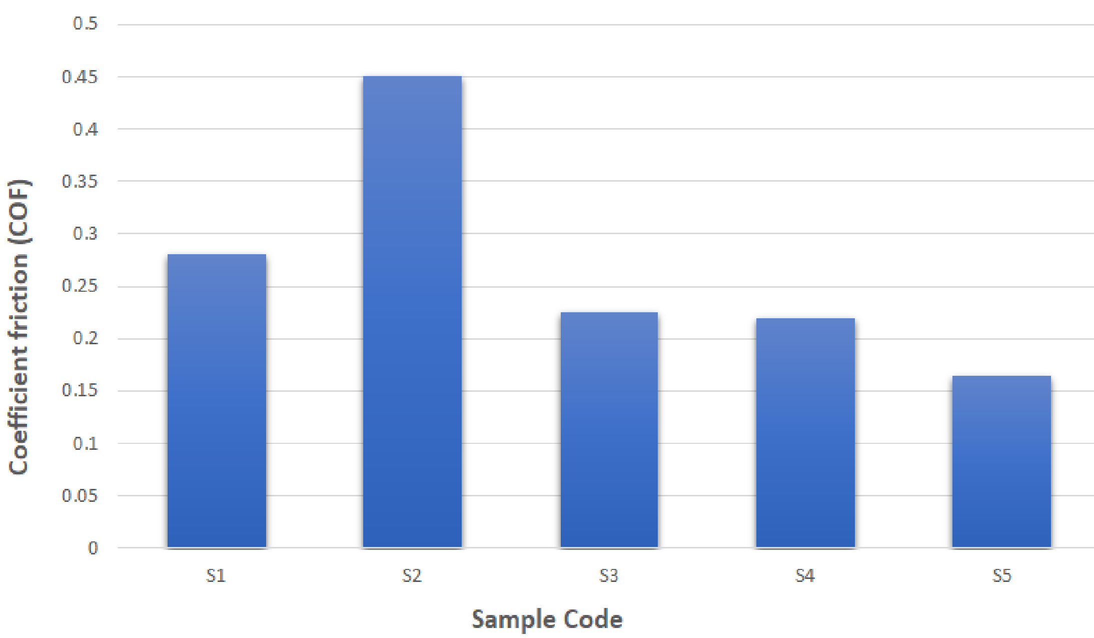

Figure 4.5 COF of Cu-Ti_3SiC_2-MoS_2-GO Composite

The wear resistance has significantly increased in the fabricated copper alloy composite, which is directly related to the increased hardness of the composite. This research work also confirms that using GO to enhance the wear properties of the composite is more recommended than using MoS_2 (B. Chen et al., 2018).

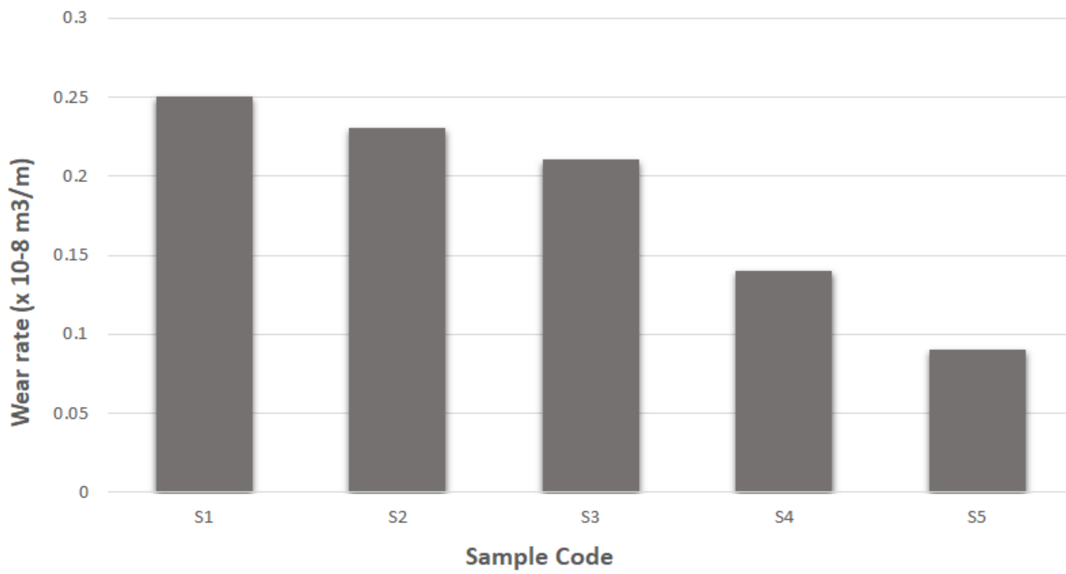

Figure 4.7 Wear rate of fabricated hybrid composite

As depicted in Figure 4.6 and Figure 4.7, the coefficients of friction as well as wear rate follow the order S3 > S4 > S5. This can be attributed to the influence of Ti_3SiC_2 MAX Phase nanoparticle reinforcement. As the weight percentage of Ti_3SiC_2 increases, the coefficient of friction and wear rate decreases.

4.6. Corrosion Test

In this test the reinforced copper composite was exposed to 3.5% NaCl solution for short time to see the corrosion effect on the samples fabricated. The corrosion current density (Icorr) and corrosion potentials (Ecorr) demonstrate a significant difference in corrosion behavior between the unreinforced composite series and the metal and ceramic reinforced composite series. In order to ensure the longevity of the material, a lower corrosion rate value is necessary. In this research work, Tafel plots are employed as a quick and easy electrochemical method. The corrosion current, obtained from the intersection of the cathodic and anodic Tafel plots' slopes, can theoretically be utilized to calculate the corrosion rate.

Table 4.6 Electrochemical corrosion for fabricated samples in 3.5% NaCl solution

Sample code	Composition	Corrosion Current (Icorr) (mA/cm^2)	Corrosion potential (Ecorr) (V)	Corrosion rate mmpy
S1	Cu15000 1%Ti3SiC2, 1%MoS2	-2.3748056	-0.23867795	0.001161314
S3	Cu15000 1%Ti3SiC2, 1%GO, 1% MoS2	-2.22728283	-0.224474187	0.001041665
S4	Cu15000 2%Ti3SiC2, 1%GO, 1% MoS2	-2.09920018	-0.234239279	0.000981006
S5	Cu15000 3%Ti3SiC2, 1%GO, 1% MoS2	-1.54837814	-0.205476646	0.000727985

(B. P. Singh et al., 2013), Investigated that the corrosion rate for Cu-GO to be 0.0025 mmpy immersed in a 3.5% NaCl solution for 30 min, which is 10 times improved than the copper bar. In this research work the result shows that there is more than 100% increment in the corrosion resistance of the manufactured copper hybrid composites. This can be attributing to the addition of Max phase in the fabricated composite.

The effect of Ti3SiC2 is shown in figure 4.8 that 1% increment of this max phase has high amount of reduction in corrosion rate in the hybrid metal matrix composite.

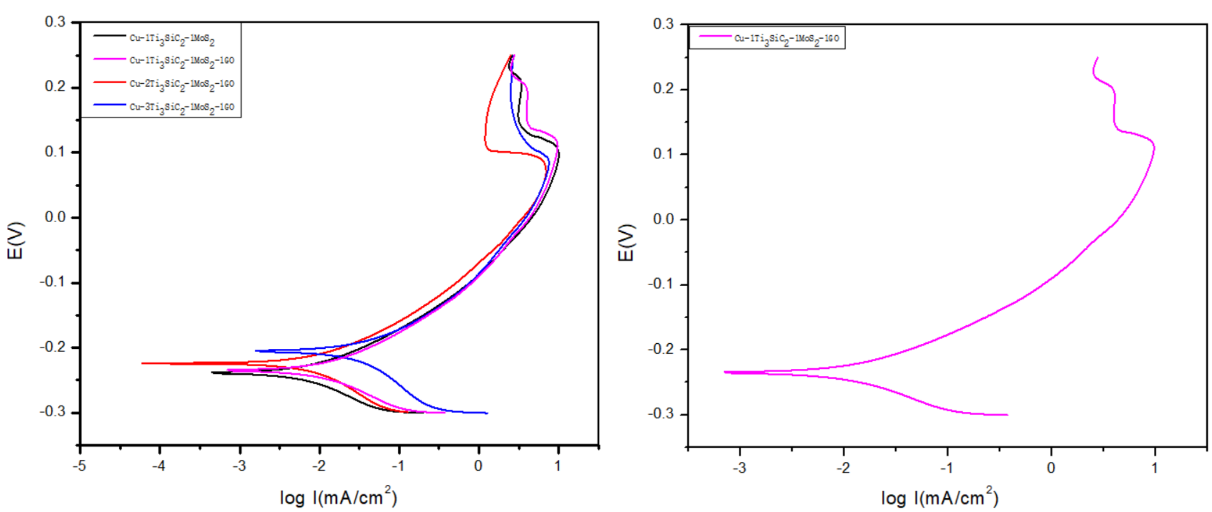

(a) (b)

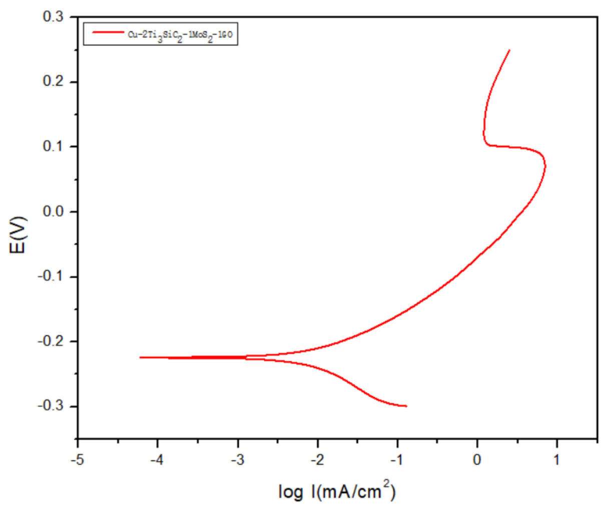

(c)

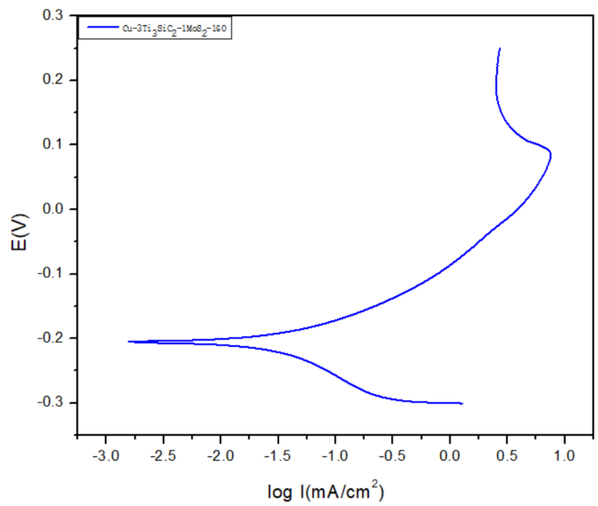

(d)

Figure 4.8 Tafel plot of copper matrix hybrid composite specimens in 3.5%NaCl solution

From the corrosion test we can also obtain Electrochemical impedance spectroscopy EIS which illustrates the electrical property of a material relative to each other.

Using EIS plot Figure 4.10 we can tell the sample with higher electrical resistance or conductive reinforcement used. Sample 5 with composition of Cu-3Ti3SiC2- 1MoS2- 1GO has the highest electrical resistance or lowest electrical conductivity since they are inversely proportional.

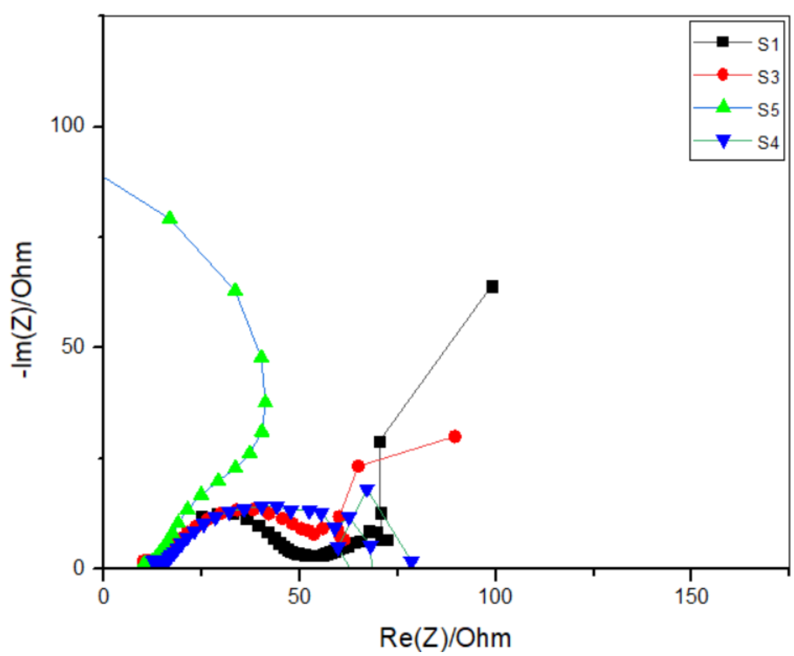

Figure 4.9 EIS plot

4.7. Electrical Conductivity Test

Electrical conductivity was recalculated using the formula indicated in equation 3.4, by measuring the resistance of the composite with a precision multimeter. The objective of the research is to improve the mechanical and tribological properties of copper by incorporating MoS2, GO and Ti3SiC2 MAX Phase. However, it its important to minimize any negative impact on the electrical properties, as the fabricated copper composite will be used for electrical applications.

Figure 4.11 shows the electrical property of copper and hybrid copper composite. For Cu, Cu 1Ti3SiC2 1MoS_2, Cu 1Ti_3SiC_2 1GO, Cu 1Ti_3SiC_2 1MoS_2 1GO, Cu 2Ti_3SiC_2 1MoS_2 1GO, and Cu 3Ti_3SiC_2 1MoS_2 1GO the electrical conductivity is 58.1, 52, 50, 48.2, 47.4, and 46.5 MS/m respectively.

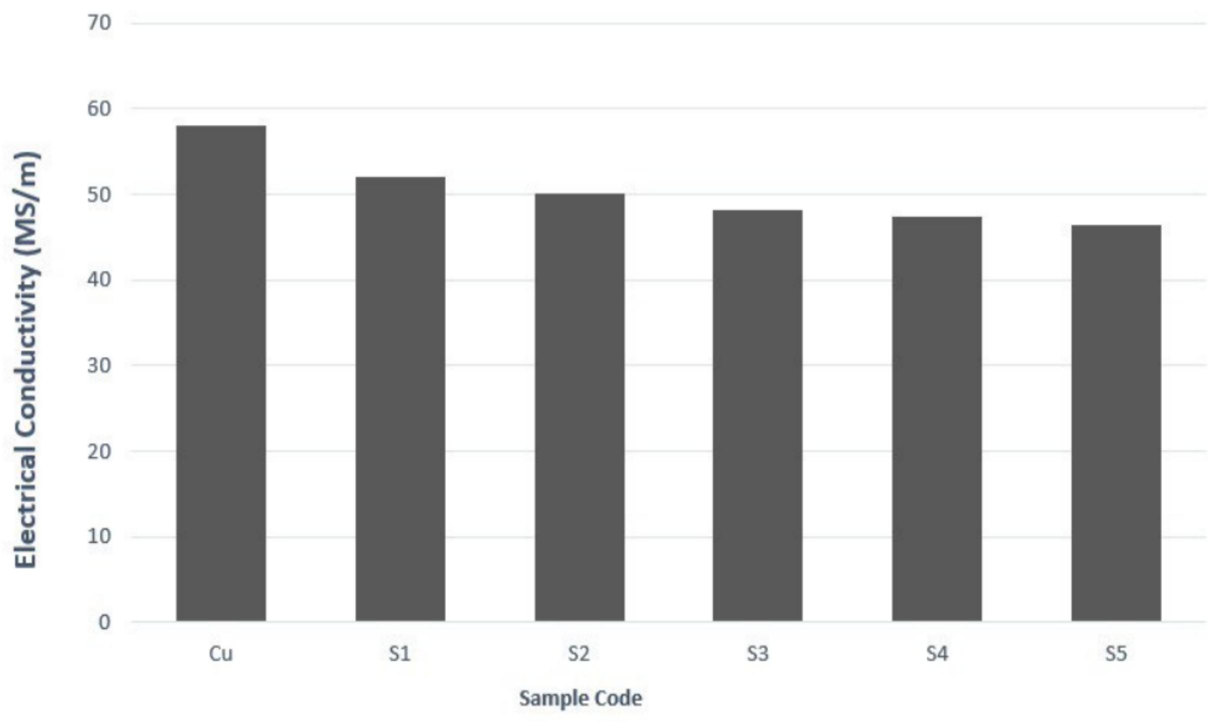

Figure 4.10 Electrical conductivity of copper hybrid composite

As it can be seen form the figure 4.10 above, even though the first two samples have similar wt. content of Ti3SiC2, S1 has higher electrical conductivity than S2. This is the result of insulator nature of GO (Phiri et al., 2018) and semiconductor nature of MoS2 (Saha & Kruse, 2020). Form

S3 to S5 increasing the wt.% of reinforcements lead to decrease in the electrical conductivity of the hybrid composite this is attribute to low electrical conductivity of reinforcements.

The addition of 20vol% of Ti3SiC2 results in electrical conductivity of 63% IASC, which is equal to 36.5 MS/m and increasing the hardness of the composite up to 121 HV (J. Chen et al., 2023). As shown in figure 4.10 above the minimum electrical conductivity of the hybrid composite is 46.5 MS/m.

4.8. Microstructural Study

During the material characterization process, the main focus was on observing the microstructure. By studying the observable patterns in the microstructures, it is possible to make informed deductions about the actual qualities of the analyzed specimens. In this study, the microstructural analysis served as confirmation for the improvement in mechanical properties resulting from the addition of reinforcement to the base metal matrix. All the synthesized specimens discussed in this study are examined in detail. The composite's phase and microstructure were examined using both optical microscopy and scanning electron microscopy.

4.8.1. Optical Microscopy

Image J was used to analyze the grain size and porosity level of a synthesized composite with varying weight percentages. Figure 4.12 shows the examination of the distribution of reinforcing particles in the copper matrix using optical microscopy (OM). The grain size was determined using imaging software with the help of an optical microscope image. The intercept approach was used to measure the grain size, resulting in a range of measurements form 27.4µm to 63.7µm, depending on the OM image. By taking five trial values form different locations on the specimen image, the average grain size was calculated to be 44.04µm.

It was investigated S5 (Cu-3Ti3SiC2-1MoS2-1GO) has finer grain size which led to have higher compression strength and mechanical hardness. This is a confirmation for the hardness and compressive strength obtained in the preceding sections.

The reason for having fine grain size of copper hybrid composites are the contribution of optimum reinforcement wt.%, the size of reinforcements (Nano particle), preheating of the reinforcement particles to provide sufficient wettability and the selection of appropriate stirring temperature, stirring speed and stirring time (Kumar et al., 2021).

Image J was used to analyze the porosity level and grain size of a synthesized composite with varying weight percentages. The calculated porosity percentages for the five samples are 3.73%, 1.98%, 2.95%, 2.56% and 2.33% respectively. These values align well with the porosity level calculated using equation (3.5).

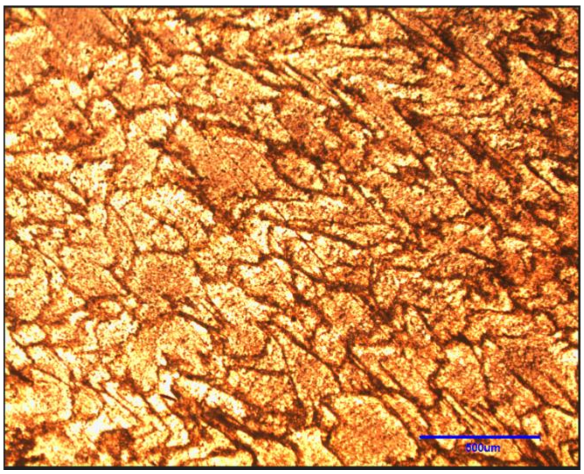

(a) Cu-1Ti3SiC2-1MoS2

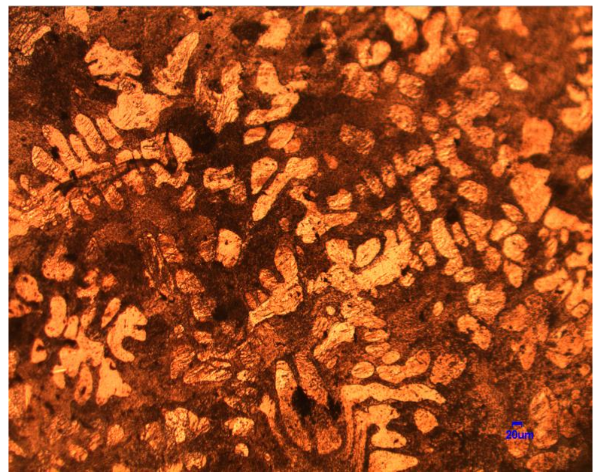

(b) Cu-1Ti3SiC2-1GO

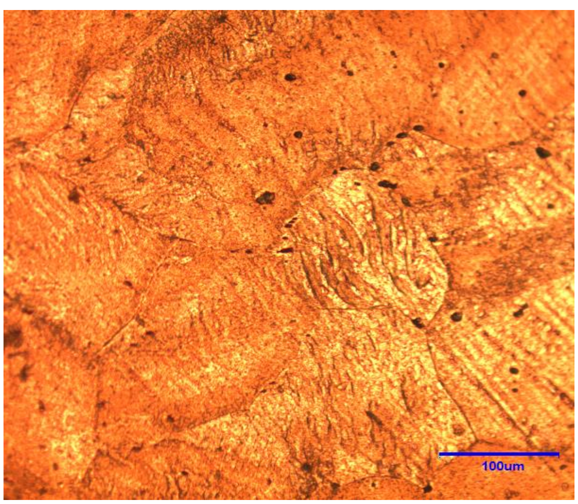

(c) Cu-1Ti3SiC2-1MoS2-1GO

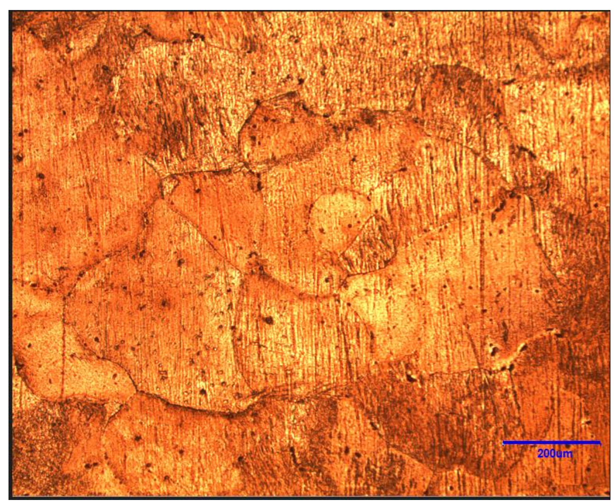

(d) Cu-2Ti3SiC2-1MoS2-1GO

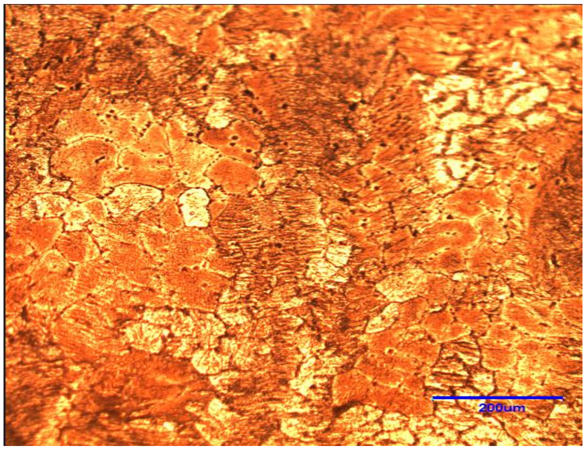

(e) Cu-3Ti3SiC2-1MoS2-1GO

Figure 4.11 Microstructure of fabricated samples using OM

The image showed that the reinforcement particles were evenly distributed throughout the base matrix Copper alloy (Cu 15000). This is likely because of the carefully chosen parameters for sample fabrication and the appropriate composite fabrication procedure. No cracks or clusters of reinforcements were observed in the image. This can be attributed to the low weight percentage of reinforcements used, with a maximum of 5% in total.

4.8.2. Scanning Electron Microscopy

The scanning electron microscope is great for studying and analyzing the surfaces of solid objects. It is advantageous to further study the topography of composite samples using SEM at different magnifications. This is because it offers higher magnification and resolution, as well as increased depth of field. Furthermore, the information obtained from an optical microscope (OM) and an SEM complement each other, providing a more comprehensive understanding of the sample.

Form the mechanical test performed (Hardness and Compression) and the confirmation obtained using optical microscopy characterization, sample five (Cu-3Ti3SiC2-1MoS2-1GO) is selected to be the best sample with enhanced mechanical strength.

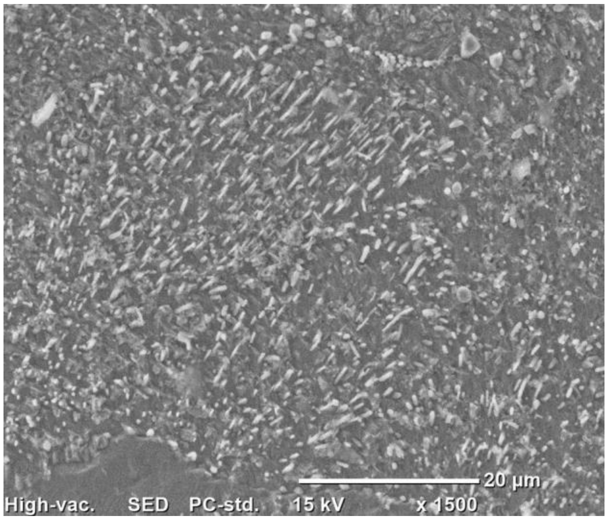

(a) x1500

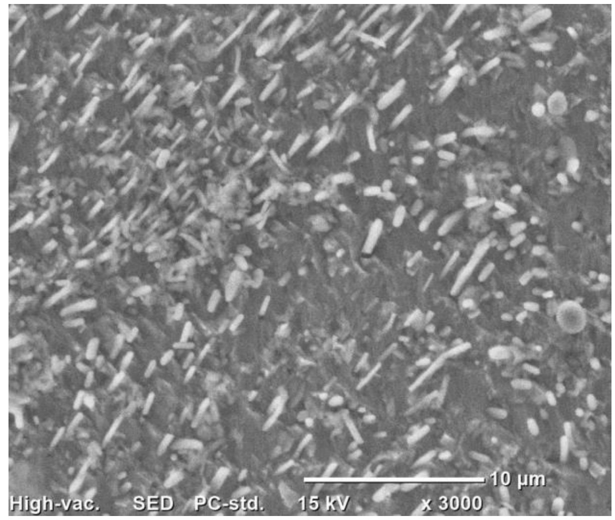

(b) x 3000

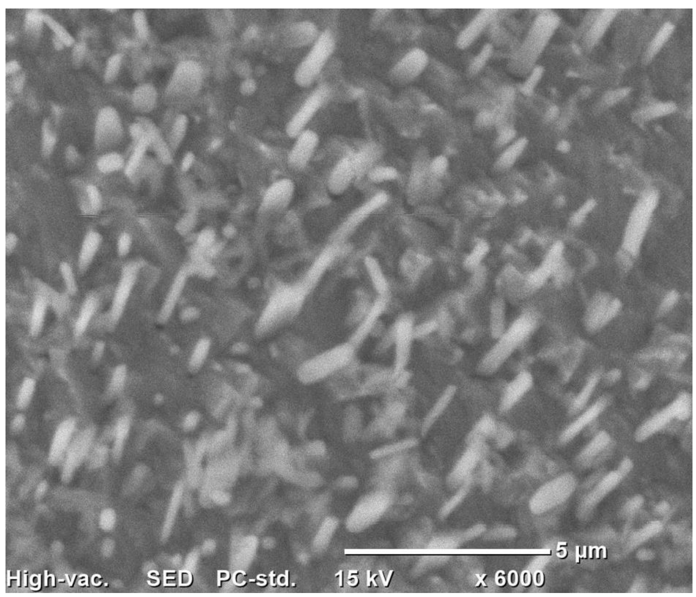

(c) x 6000

Figure 4.12 SEM result of selected sample in different magnification

Figure 4.12 depicts the SEM observations of copper metal matrix composite samples, which reveal the well distribution of particles on the base metal with the average grain size of 800nm.

4.8.3. X-Ray Diffraction analysis

The XRD pattern of the Cu composites containing 2, 3, 4, and 5 wt.% of total reinforcement composites reveals the elements present in the composites, as shown in figure 4.14. The composition of the composite was determined through XRD analysis. Based on the XRD pattern of the composite samples, peaks corresponding to Titanium silicon carbide (Ti3SiC2), Molybdenum disulfide (MoS2), and GO were detected among the identified compound phases.

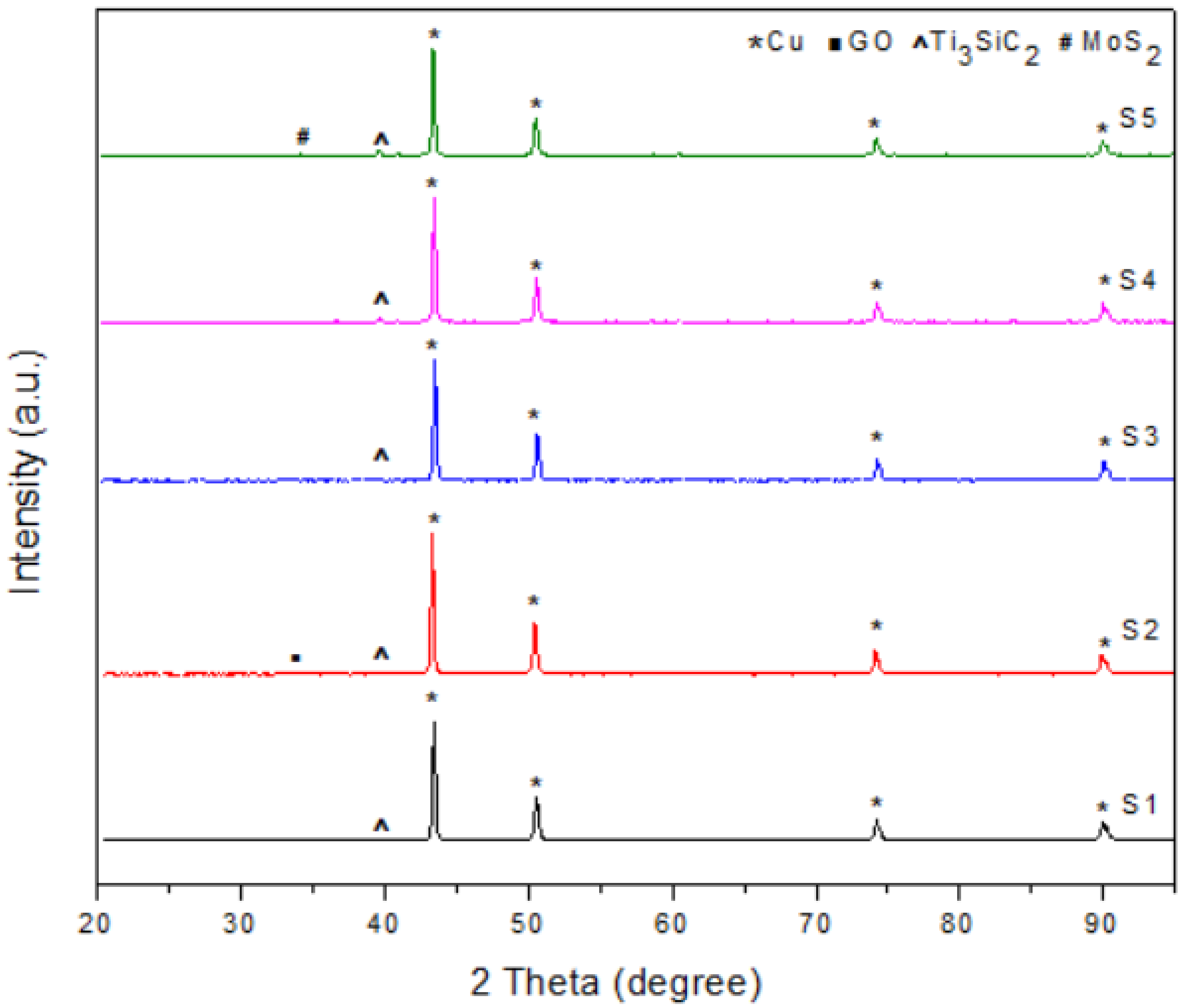

Figure 4.13 XRD spectrums of fabricated samples at different reinforcement compositions.

4.8.4. FTIR Spectroscopy

Characterization of a vibration Cu-MoS_2-GO-Ti_3SiC_2 vibration is shown in Figure 4.15, in the range of 4000-400 cm-1 wavelengths. The spectrum of Cu-MoS2-GO-Ti3SiC2 gave the absorption spectra of Si-Compound at 2163cm-1, C=O at 1725 cm-1, C-OH at 1355 cm^{-1}, and C-H at 1214 cm^{-1} for all the five samples. For Cu-1MoS_2-1GO-2Ti_3SiC_2 gave additional absorption spectra of Mo-S at 597 cm^{-1} and –CH at 2898 cm^{-1}. For Cu-1MoS_2-1Ti_3SiC_2 also there are additional absorption spectra of Mo-S at absorption spectra of Mo-S at 597 cm^{-1}. The results align with the research conducted on Cu, MoS_2, GO, and Ti_3SiC_2 (Amini et al., 2019; Han et al., 2017; Maria & Goerne, 2016; Rochman et al., 2019; Vaisakh et al., 2015; Vinoth et al., 2016).

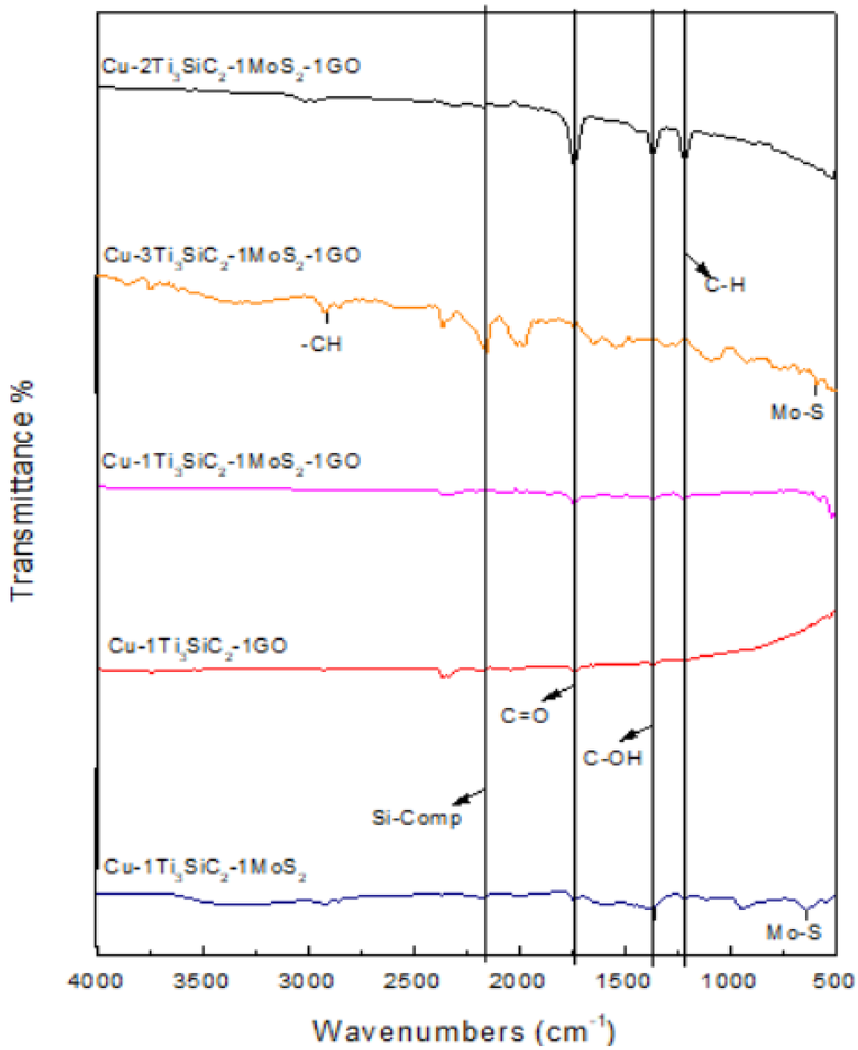

Figure 4.14 FTIR graph for copper hybrid composite

These give an evidence for the synergetic effect of reinforcements in the fabricated compounds observed form the mechanical and tribological test results. The reinforcement particles have successfully entered the copper structure giving new composite with enhanced physical, mechanical and tribological properties.

4.9. Optimization using Taguchi based Grey Relational Analysis

To identify the best sample composition for achieving the highest quality copper composite metal matrix, a comprehensive dataset was created by combining data from tests measuring porosity, hardness, wear rate, compression strength, and signal-to-noise ratios of COF.

Step 1: Determine the S/N ratio for the matching answers by applying Equations 3.2, 3.3, and 3.4.

Step 2: Using Eq. 3.6, a grey connection that ranges from 0 to 1 is created during the normalization of the S/N values.

4.9.1. Signal to noise ratio of the experiment values

The characteristics of measurements are crucial for improving signals while considering uncontrollable variables, aiming to minimize noise in the response results. This lead to optimal properties in the anticipated composite product. The criteria include "smaller the better," "nominal value the better" and "the larger the better."

Table 4.7 S/N ratios of experimental values

	S/N ratios				
Run	Porosity	Hardness	Wear rate	Compression Strength	COF
S1	-11.005	47.664	12.041	51.976	12.041
S2	-5.249	49.824	12.765	51.246	6.936
S3	-9.036	50.076	13.556	53.497	12.956
S4	-7.082	50.806	17.077	54.387	13.152
S5	-6.486	51.576	20.915	54.648	15.65

For this reason the statistical formula "smaller the better" is used for porosity, wear rate and COF, where as "the larger the better" is used for hardness and compression. The S/N rations for each response were illustrated in table 4.5.

4.9.2. Normalizing the experimental values

In this stage, the data derived from the S/N ration is normalized to standardize it for subsequent analysis, thereby removing the impact of variability and varying units.

Hence, the S/N ratio values obtained from all experimental runs are normalized to fall within the range of 0 to 1 using equation 3.11 and 3.12, as detailed in the earlier chapter. The resulting transformed values for the response are presented in table 4.8.

Table 4.8 Normalized data of experimental values

Experimental Run's	Normalization value				
	Porosity	Hardness	Wear rate	Compression strength	COF
S1	-1	0	-1	0.183	0.298
S2	0	0.496	-0.875	0	1
S3	-0.581	0.563	-0.75	0.617	0.211
S4	0.121	0.766	-0.313	0.909	0.193
S5	-0.163	1	0	1	0

4.9.3. Grey relational coefficient and Grey relational grades

The process of converting the response data into a signal response for additional analysis led to the determination of the gray relational coefficients (GRCs). Equation 3.13 is used to generate GRCs by establishing the link between real and experimental data using the normalized S/N ratio data. Table 4.9 displays the deviation sequence values for every answer along with the matching GRC values. After that, a single answer is created from the highest and minimum values using equation 3.14, often known as the Grey Relation Grade (GRG). From these, the first rank from the five experimental runs is given to the one with the greatest GRG value, and the last rank is given to the one with the lowest. Because it has the greatest GRG values among the five experimental runs, experimental run number five is given the first rank. Based on the results of this experiment, the level of process parameters that yields the best results is A1B3C1D2. Meanwhile, using the primary impact table 4.10, as indicated below, the mean value of GRG is used to determine influential elements and the best level combination from each process parameter.

Table 4.9 Deviation value of normalized S/N ratio

Deviation Sequence					Grey relational coefficient				
Porosity	Hardness	Wear rate	Compression	COF	Porosity	Hardness	Wear rate	Compression	COF
2	1	2	0.817	0.7	0.2	0.333	0.2	0.38	0.416
1	0.504	1.875	1	0	0.333	0.498	0.211	0.333	1
1.581	0.437	1.75	0.383	0.79	0.24	0.533	0.222	0.566	0.388
0.879	0.234	1.313	0.091	0.81	0.363	0.681	0.276	0.845	0.383
1.163	0	1	0	1	0.301	1	0.333	1	0.333

The main effect table has helped us determine the optimal levels of the parameters based on the responses. For copper, the optimal level is 1. For Ti3SiC2, the optimal level is 3. For MoS2, the optimal level is 1. And for GO, the optimal level is 2. Consequently, the optimal combination of wt. % parameters has been found to be A1B3C1D2 based on the results from the tests performed.

Table 4.10 Response table for a mean of GRG

Level	**Cu**	**Ti3SiC2**	**MoS2**	**GO**
1	**0.5930**	0.3903	**0.4750**	0.3060
2	0.5100	0.5100	0.4497	**0.4920**
3	0.3900	**0.5930**	-	-
4	0.3905	-	-	-
Delta	0.2030	0.2027	0.0252	0.1860
Rank	1	2	4	3

Figure 4.15 demonstrate the ranks and GRG values indicating the 5th sample with a composition of reinforcement 3wt.% Ti_3SiC_2, 1wt.% MoS_2 and 1wt.%GO is to be selected as the optimum sample.

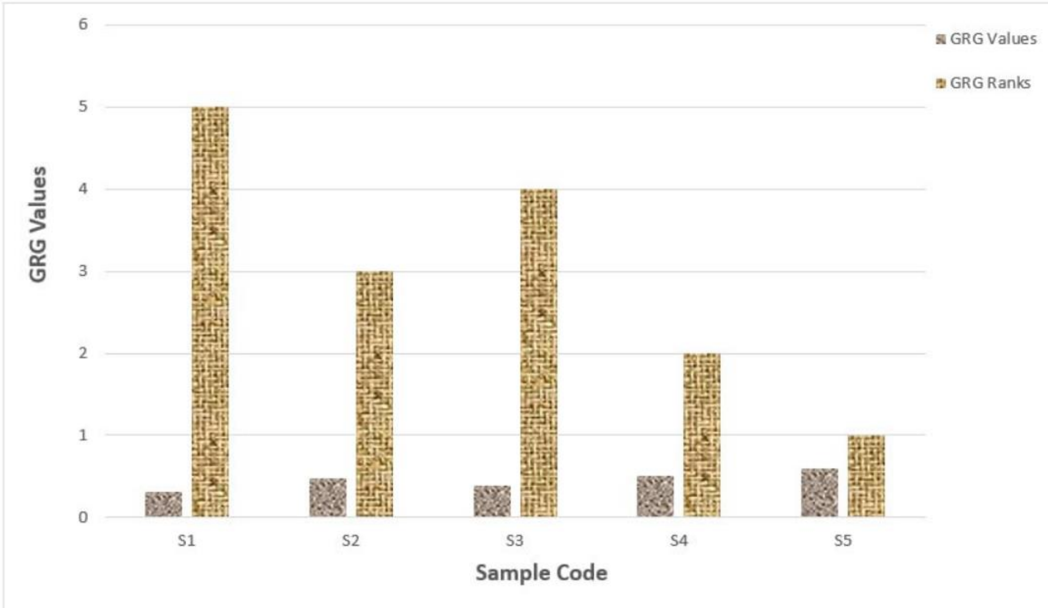

Figure 4.15 Ranks and values of GRG

4.10. Analysis of wear morphology

In this study, we also examined the wear morphology of a Copper metal matrix composite by conducting a wear test using a pin on disc apparatus. A 30N applied load was used. The SEM characterizing tool was used to investigate the worn surface of optimum sample. The results showed various wear mechanisms, including continuous grooves, wear debris, delamination, and scratches. These wear mechanisms were mainly observed along the sliding directions this is as a result of the applied force form the tip of the tester on the specimen. Figure 4.16 clearly illustrates that abrasive wear and fatigue wear mechanisms were the most common in the samples. The SEM micrographs of the worn surfaces confirmed that the wear resistance was improved due to the presence of GO and Ti_3SiC_2. Additionally, the addition of molybdenum disulfide (MoS_2) helped to reduce wear loss by promoting the uniform distribution of particles over the matrix materials. Previous literature (Ismail et al., 2021; L. Wang et al., 2023), also reported that composites manufactured with the inclusion of Ti_3SiC_2 and solid lubricants exhibited a reduction in wear losses.

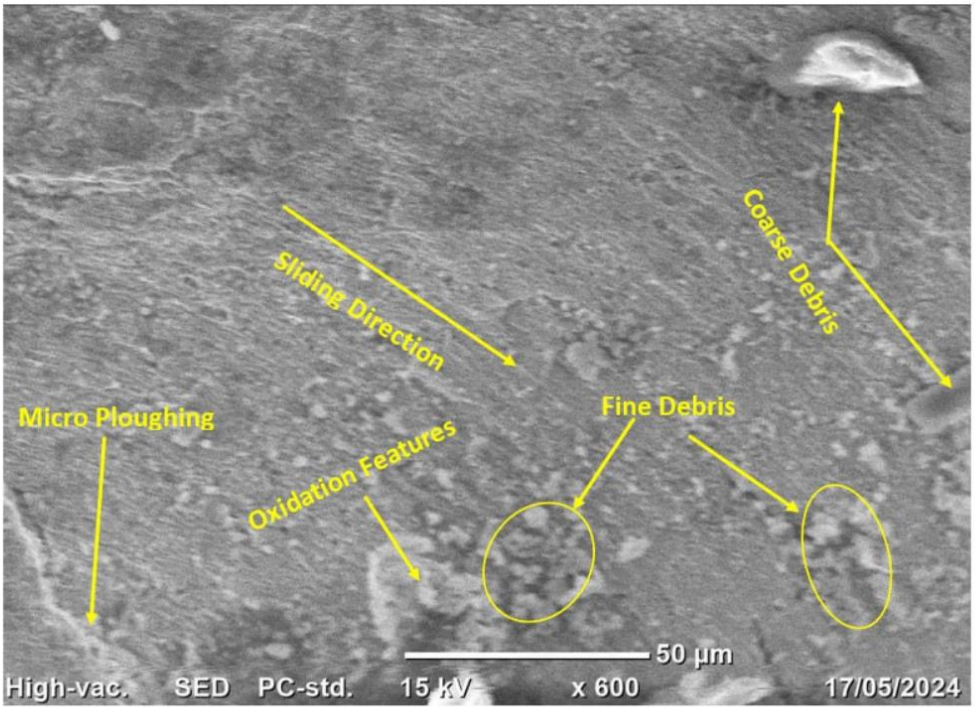

Figure 4.16 SEM micrograph of wear morphology of optimal sample

CHAPTER FIVE

CONCLUSION AND RECOMMENDATION

5.1. Conclusion

The aim of this research work was to successfully manufacture copper hybrid composites using the stir casting manufacturing technique. Five copper composite samples are fabricated using stir casting technique having reinforcement wt. % of $1Ti_3SiC_2$-$1MoS_2$, $1Ti_3SiC_2$-1GO, $1Ti_3SiC_2$-$1MoS_2$-1GO, $2Ti_3SiC_2$-$1MoS_2$-1GO and $2Ti_3SiC_2$-$1MoS_2$-1GO for S1, S2, S3, S4 and S5 respectively. The study also investigated the effect of liquid metallurgy process parameters and the weight percentage of selected reinforcements. Through an analysis of existing research, the optimum combination of process parameters was determined to achieve an average property. Additionally, the hybrid composite was thoroughly characterized, leading to the following conclusions:

- ✓ Density and porosity measurement shows that density of the fabricated hybrid composite is to be measured 8.43, 8.52, 8.37, 8.34 and 8.27g.cm^3 for S1, S2, S3, S4 and S5 respectively. The theoretical as well as actual density of the composite decreases as the wt. % of reinforcement increases. And this is due to lower density of reinforcing materials and the presence of porosity. The porosity level of the composite is to be found in between 1.83-3.55% which arised form presence of impurities and void in the fabricated sample during fabrication process, however low amount of porosity indicates proper selection of stir casting parameters.
- ✓ The compressive strength of fabricated hybrid copper metal matrix composite has increased up to 83% which is very high increment applying only up to 5 wt. % of total reinforcement materials.
- ✓ Wear rate and coefficient of friction test were performed using pin on disk load of 30N at 300rpm for 10 min, the result obtained from all the fabricated sample is very low compare to the base metal. Wear rate was to be found 0.22 x $10^{-8}m^3/m$ for second sample containing only GO and Ti_3SiC_2 reinforcements which is lower than that of S1, indicating GO has more wear rate reduction impact than MoS_2 whereas the COF of friction is lower for S1 amounting 0.28 indicating that MoS_2 has higher COF reduction capacity than GO. Additionally, from the entire tested samples sample five containing both the GO and MoS_2

reinforcements and 3% Ti_3SiC_2 have the least wear rate (0.09 x $10^{-8}m^3/m$) and COF (0.165) showing better tribological capacity of Ti_3SiC_2.

- ✓ Under 3.5% NaCl solution corrosion test, corrosion rate of 0.000727985 mm/year was obtained from the fifth sample. This result demonstrates the highest corrosion resistance capacity of Cu-2Ti_3SiC_2-1MoS_2-1GO.
- ✓ The electrical conductivity test calculated using resistance value of the fabricated samples using multimeter are 58.1, 52, 50, 58.2, 47.4 and 46.5 MS/m for S1, S2, S3, S4, and S5 respectively. These results show the reducing effect of reinforcements and increased wt. % in the electrical conductivity of copper alloy. Through enhancing mechanical and microstructural properties of copper the electrical conductivity reduction is not too much for all the five samples fabricated promising that these materials can be used in the application of electrically conductive equipment's.
- ✓ The microstructural study using of OM and SEM shows the uniform distribution of reinforcements in the base metal matrix having average grain size of 44.04μm and approximately equal amount of experimental porosity level (3.73%, 1.98%, 2.95%, 2.56% and 2.33% respectively for the 5 samples for S1 to S5) as it was calculated using density measurement. Smaller grain size and low-level porosity identified in the characterization of the samples using OM and SEM, is to be found the main reasons for the enhanced mechanical properties mentioned above.
- ✓ XRD analysis result shows the finger print of the composition including all the reinforced nanoparticles. Application of small number of reinforcing particles in the fabricated samples exhibits low weight percentage of reinforcement peaks.
- ✓ Characterization of vibration using FTIR spectrum gave absorption of Cu-MoS2-GO-Ti3SiC2 gave the absorption spectra of Si-Compound, C=O, C-OH, and CH for all the five samples. For Cu-1MoS2-1GO-2Ti3SiC2 gave additional absorption spectra of Mo-S and –CH. For Cu-1MoS2-1Ti3SiC2 also there are additional absorption spectra of Mo-S functional groups indicating the synergetic effect of reinforcement in the fabricated samples giving new composition with enhanced physical, mechanical and tribological properties.
- ✓ From gray relation analysis the optimal sample for this research is selected a metal matrix with composition of 95% Cu-3%Ti3SiC2-1%MoS2-1%GO.

- ✓ The wear morphology studied using SEM on the optimized sample result suggest that abrasive and adhesive wear are mainly observed.

5.2. Recommendation

In this study, a copper alloy metal matrix composite is manufactured with five different reinforcement compositions. The purpose is to determine its mechanical properties (hardness and compressive strength), tribological properties (wear resistance and corrosion resistance), and electrical properties (recomputed using resistance value extracted form multimeter). The composite is characterized using various tools to examine its microstructural properties. Based on the result and conclusions, it its recommended that The fabricated copper alloy metal composite, can be used in electrical application specifically for bus bar. This is because it exhibits enhanced mechanical strength and higher corrosion, and wear resistance compared to commercial copper and its alloys. To further study the properties of the produced composite, it is suggested to fabricate more samples with a wide range of wt. % and perform additional tests such as tensile strength, impact, thermal and other tests to investigate more its mechanical, tribological, and thermal properties of the manufactured metal matrix composites (MMMCs). The result implies that both the material and manufacturing techniques play a crucial role in obtaining the desired properties of the composites. Therefore, the use of highly effective tools is recommended to overcome difficulties during manufacturing and testing the samples. Furthermore, it is also recommended to perform secondary operation on the manufactured samples in order to further enhance the properties of the metal matrix.

Research Fund Acknowledgement

This research project is funded by Adama Science and Technology University under the grant number ASTU/SM-R/1046/24, Adama, Ethiopia.

References

Aatthisugan, I., Rose, A. R., & Jebadurai, D. S. (2017). Mechanical and wear behaviour of AZ91D magnesium matrix hybrid composite reinforced with boron carbide and graphite. *Journal of Magnesium and Alloys*, *5*(1), 20–25.

Abebe Emiru, A., Sinha, D. K., Kumar, A., & Yadav, A. (2023). Fabrication and Characterization of Hybrid Aluminium (Al6061) Metal Matrix Composite Reinforced with SiC, B4C and MoS2 via Stir Casting. *International Journal of Metalcasting*, *17*(2), 801–812. https://doi.org/10.1007/s40962-022-00800-1

Abilash, N., & Sivapragash, M. (2016). Optimizing the delamination failure in bamboo fiber reinforced polyester composite. *Journal of King Saud University - Engineering Sciences*, *28*(1), 92–102. https://doi.org/10.1016/j.jksues.2013.09.004

Ali, M. A., Hossain, M. M., Uddin, M. M., Hossain, M. A., Islam, A. K. M. A., & Naqib, S. H. (2021). Physical properties of new MAX phase borides M2SB (M = Zr, Hf and Nb) in comparison with conventional MAX phase carbides M2SC (M = Zr, Hf and Nb): Comprehensive insights. *Journal of Materials Research and Technology*, *11*, 1000–1018. https://doi.org/10.1016/j.jmrt.2021.01.068

Amini, M., A, A. R. S., & Kheradmand, A. (2019). In-Situ Polymerization of UHMWPE Using Bi - Supported Ziegler-Natta Catalyst of MoS 2 Oxide / MgCl 2 (Ethoxide Type)/ TiCl 4 / TiBA : Study of Thermo- Mechanical Properties of System. *Int. J. New. Chem.*, *6*(2), 87–108.

Ankur, Bharti, A., Prasad, D., Kumar, N., & Saxena, K. K. (2021). A Re-investigation: Effect of various parameter on mechanical properties of copper matrix composite fabricated by powder metallurgy. *Materials Today: Proceedings*, *45*, 4595–4600. https://doi.org/10.1016/j.matpr.2021.01.009

Arunachalam, R., Kumar, P., & Muraliraja, R. (2019). *A review on the production of metal matrix composites through stir casting – Furnace design , properties , challenges , and research opportunities*. *42*(September 2018), 213–245. https://doi.org/10.1016/j.jmapro.2019.04.017

Bansal, P., & Upadhyay, L. (2016). Effect of Turning Parameters on Tool Wear, Surface

Roughness and Metal Removal Rate of Alumina Reinforced Aluminum Composite. *Procedia Technology*, *23*, 304–310. https://doi.org/10.1016/j.protcy.2016.03.031

Beb, M. Y., Dembélé, S., Bekel, A., Jouffroy-Bapicot, I., Thibaud, S., Piat, N., Lehmann, O., Rauch, J.-Y., Rougeot, P., & Lebas, L.-M. (2022). Proposal for a complete 3D surface reconstruction using images from a scanning electron microscope (SEM). *Laser Science*, JW5A-69.

Chen, B., Li, X., Jia, Y., Xu, L., Liang, H., Li, X., Yang, J., Li, C., & Yan, F. (2018). Fabrication of ternary hybrid of carbon nanotubes/graphene oxide/MoS2 and its enhancement on the tribological properties of epoxy composite coatings. *Composites Part A: Applied Science and Manufacturing*, *115*(September), 157–165. https://doi.org/10.1016/j.compositesa.2018.09.021

Chen, J., Ye, F., Cheng, L., Yang, J., & Chen, X. (2023). Preparation and properties of Ti3SiC2 preform reinforced SiC ceramic matrix composites. *Journal of the European Ceramic Society*, *43*(8), 3146–3157.

Das, B., Roy, S., Rai, R. N., Saha, S. C., & Majumder, P. (2016). Effect of in-situ processing parameters on microstructure and mechanical properties of TiC particulate reinforced Al–4.5Cu alloy MMC fabricated by stir-casting technique – Optimization using grey based differential evolution algorithm. *Measurement: Journal of the International Measurement Confederation*, *93*, 397–408. https://doi.org/10.1016/j.measurement.2016.07.044

Dinaharan, I., & Albert, T. (2023). Effect of reinforcement type on microstructural evolution and wear performance of copper matrix composites via powder metallurgy. *Materials Today Communications*, *34*, 105250.

Dmitruk, A., & Naplocha, K. (2022). DEVELOPMENT OF Al-Ti-C POROUS STRUCTURES FOR REINFORCING ALUMINUM MATRIX COMPOSITES. *Composites Theory and Practice*, *2022*(3), 172–177.

Gautam, Y. K., Somani, N., Kumar, M., & Sharma, S. K. (2018). A review on fabrication and characterization of copper metal matrix composite (CMMC). *AIP Conference Proceedings*, *2018*(Cmmc). https://doi.org/10.1063/1.5058254

Gonfa, B. K., Sinha, D., Vates, U. K., Badruddin, I. A., Hussien, M., Kamangar, S., Singh, G. K., Ahmed, G. M. S., Kanu, N. J., & Hossain, N. (2022). Investigation of mechanical and tribological behaviors of aluminum based hybrid metal matrix composite and multi-objective optimization. *Materials*, *15*(16), 5607.

Gonzalez-Julian, J. (2021). Processing of MAX phases: From synthesis to applications. *Journal of the American Ceramic Society*, *104*(2), 659–690. https://doi.org/10.1111/jace.17544

Grieseler, R., Camargo, M. K., Hopfeld, M., Schmidt, U., Bund, A., & Schaaf, P. (2017). Copper-MAX-phase composite coatings obtained by electro-co-deposition: A promising material for electrical contacts. *Surface and Coatings Technology*, *321*, 219–228. https://doi.org/10.1016/j.surfcoat.2017.04.060

Groover, M. P. (2020). *Fundamentals of modern manufacturing: materials, processes, and systems*. John Wiley & Sons.

Guler, O., & Bagci, N. (2020). A short review on mechanical properties of graphene reinforced metal matrix composites. *Journal of Materials Research and Technology*, *9*(3), 6808–6833. https://doi.org/10.1016/j.jmrt.2020.01.077

Hallem, A. H., & Dawood, N. M. (2018). Investigation the effects of zirconium addition on wear and corrosion behaviour of α-brass alloy (Cu-Zn30). *International Journal of Mechanical Engineering and Technology*, *9*(844–857), 844–857.

Han, S., Liu, K., Hu, L., Teng, F., Yu, P., & Zhu, Y. (2017). Superior Adsorption and Regenerable Dye Adsorbent Based on Flower-Like Molybdenum Disulfide Nanostructure. *Scientific Reports*, *7*(March), 1–11. https://doi.org/10.1038/srep43599

Huang, J., Yan, X., Chang, C., Xie, Y., Ma, W., Huang, R., Zhao, R., Li, S., Liu, M., & Liao, H. (2020). Pure copper components fabricated by cold spray (CS) and selective laser melting (SLM) technology. *Surface and Coatings Technology*, *395*(March), 125936. https://doi.org/10.1016/j.surfcoat.2020.125936

Ismail, N. A., Chowdhury, Z. Z., Johan, M. R., & Zulkifli, N. W. M. (2021). MoS2-functionalized graphene composites—Potential replacement for lubricant friction modifier and anti-wear additives. *Advanced Engineering Materials*, *23*(9), 2100030.

Jahani, A., Aval, H. J., Rajabi, M., & Jamaati, R. (2023). Effects of Ti2SnC MAX phase reinforcement content on the properties of copper matrix composite produced by friction stir back extrusion process. *Materials Chemistry and Physics*, *299*, 127497.

Jamwal, A., Seth, P. P., Kumar, D., Agrawal, R., Sadasivuni, K. K., & Gupta, P. (2020). Microstructural, tribological and compression behaviour of Copper matrix reinforced with Graphite-SiC hybrid composites. *Materials Chemistry and Physics*, *251*, 123090. https://doi.org/10.1016/j.matchemphys.2020.123090

Jha, P., Joshi, K. K., & Routara, B. C. (2021). *Process parameters optimization in CNC turning of aluminum 7075 alloy using TOPSIS method coupled with Taguchi philosophy*.

Kumar, M. S., Begum, S. R., Pruncu, C. I., & Shahedi Asl, M. (2021). Role of homogeneous distribution of SiC reinforcement on the characteristics of stir casted Al–SiC composites. *Journal of Alloys and Compounds*, *869*, 159250. https://doi.org/10.1016/j.jallcom.2021.159250

Liu, Y., Chen, X., Li, J., & Luo, J. (2019). Enhancement of friction performance enabled by synergetic effect between graphene oxide and molybdenum disulfide. *Carbon*, *154*, 266–276. https://doi.org/10.1016/j.carbon.2019.08.009

Madhukar, P., Selvaraj, N., Gujjala, R., & Rao, C. S. P. (2019). Production of high performance AA7150-1% SiC nanocomposite by novel fabrication process of ultrasonication assisted stir casting. *Ultrasonics Sonochemistry*, *58*, 104665. https://doi.org/10.1016/j.ultsonch.2019.104665

Mang, T., Bobzin, K., & Bartels, T. (2011). *Industrial tribology: Tribosystems, friction, wear and surface engineering, lubrication*. John Wiley & Sons.

Maria, T., & Goerne, L. (2016). *Sol-gel synthesis in the presence of ZrO2 and Cu / ZrO2 . G . Fetter , P . Bosch , Tessy López , R . Gómez , Magazine of the XV Ibero-American Symposium for ZrO 2 and Cu / ZrO 2 Sol – Gel Materials Spectroscopic Characterization*. *August 1998*.

Mclinden, M. O. (2014). CHAPTER 2. Experimental Techniques 1: Direct Methods. *Volume Properties*, 73–99. https://doi.org/10.1039/9781782627043-00073

Mohan, E., Anbuchezhiyan, G., Pugazhenthi, R., & Prakash, F. P. (2023). Wear behavior of brass based composite reinforced with SiC and produced by stir casting process. *Materials Research*, *26*, e20220196.

Muramatsu, N., Kimura, H., & Inoue, A. (2013). Microstructures and mechanical properties of highly electrically conductive Cu0.5, Cu1 and Cu2at% Zr alloy wires. *Materials Transactions*, *54*(2), 176–183. https://doi.org/10.2320/matertrans.M2012264

Nagavally, R. R. (2016). Composite Materials - History, Types, Fabrication Techniques, Advantages, and Applications. *International Journal of Mechanical And Production Engineering*, *2*, 25–30.

Nautiyal, H., Kumari, S., Khatri, O. P., & Tyagi, R. (2019). Copper matrix composites reinforced by rGO-MoS2 hybrid: Strengthening effect to enhancement of tribological properties. *Composites Part B: Engineering*, *173*, 106931.

Nazeer, F., Ma, Z., Gao, L., Wang, F., Khan, M. A., & Malik, A. (2019). Thermal and mechanical properties of copper-graphite and copper-reduced graphene oxide composites. *Composites Part B: Engineering*, *163*, 77–85. https://doi.org/10.1016/j.compositesb.2018.11.004

Nee, A. Y. C. (2014). *Handbook of manufacturing engineering and technology*. Springer Publishing Company, Incorporated.

Patel GC, M., Chate, G. R., Parappagoudar, M. B., Gupta, K., Patel GC, M., Chate, G. R., Parappagoudar, M. B., & Gupta, K. (2020). Studies on Machining of Hard Materials. *Machining of Hard Materials: A Comprehensive Approach to Experimentation, Modeling and Optimization*, 25–51.

Phiri, J., Johansson, L.-S., Gane, P., & Maloney, T. (2018). A comparative study of mechanical, thermal and electrical properties of graphene-, graphene oxide-and reduced graphene oxide-doped microfibrillated cellulose nanocomposites. *Composites Part B: Engineering*, *147*, 104–113.

Pratik, A., Biswal, S. K., & Haridoss, P. (2020). Impact of enhanced interfacial strength on physical, mechanical and tribological properties of copper/reduced graphene oxide composites: Microstructural investigation. *Ceramics International*, *46*(14), 22539–22549. https://doi.org/10.1016/j.ceramint.2020.06.014

Rajak, D. K., Pagar, D. D., Kumar, R., & Pruncu, C. I. (2019). Recent progress of reinforcement materials: a comprehensive overview of composite materials. *Journal of Materials*

Research and Technology, *8*(6), 6354–6374.

Rochman, R. A., Wahyuningsih, S., Ramelan, A. H., & Hanif, Q. A. (2019). Preparation of nitrogen and sulphur Co-doped reduced graphene oxide (rGO-NS) using N and S heteroatom of thiourea. *IOP Conference Series: Materials Science and Engineering*, *509*(1). https://doi.org/10.1088/1757-899X/509/1/012119

Sabzevari, M., Sajjadi, S. A., & Moloodi, A. (2016). Physical and mechanical properties of porous copper nanocomposite produced by powder metallurgy. *Advanced Powder Technology*, *27*(1), 105–111.

Saha, D., & Kruse, P. (2020). Editors' choice—review—conductive forms of MoS2 and their applications in energy storage and conversion. *Journal of The Electrochemical Society*, *167*(12), 126517.

Salman, S. D., & Leman, Z. B. (2018). Physical, Mechanical and Ballistic Properties of Kenaf Fiber Reinforced Poly Vinyl Butyral and Its Hybrid Composites. In *Natural Fiber Reinforced Vinyl Ester and Vinyl Polymer Composites: Development, Characterization and Applications*. Elsevier Ltd. https://doi.org/10.1016/B978-0-08-102160-6.00013-5

Shankar, M. C. G., Shettar, M., Sharma, S. S., & Kini, A. (2018). Enhancement in hardness and influence of artificial aging on stir cast Al6061-B4C and Al6061-SiC composites. *Materials Today: Proceedings*, *5*(1), 2435–2443.

Sharma, A., & Porwal, R. K. (2023). *COMPOSITES-A REVIEW*. *12*(Mmc), 2383–2389. https://doi.org/10.31838/ecb/2023.12.3.178

Shi, C.-L., & Butenko, M. A. (2018). Visualizing morphological changes of abscission zone cells in Arabidopsis by scanning electron microscope. *Plant Senescence: Methods and Protocols*, 321–328.

Singh, B. P., Nayak, S., Nanda, K. K., Jena, B. K., Bhattacharjee, S., & Besra, L. (2013). The production of a corrosion resistant graphene reinforced composite coating on copper by electrophoretic deposition. *Carbon*, *61*, 47–56. https://doi.org/10.1016/j.carbon.2013.04.063

Singh, M. K., Gautam, R. K., & Ji, G. (2019). Mechanical properties and corrosion behavior of copper based hybrid composites synthesized by stir casting. *Results in Physics*, 102319. https://doi.org/10.1016/j.rinp.2019.102319

Somani, N., Tyagi, Y. K., Kumar, P., Srivastava, V., & Bhowmick, H. (2018). Enhanced tribological properties of SiC reinforced copper metal matrix composites. *Materials Research Express*, *6*(1), 16549.

Srimurugan, R., Vijay Ananth, S., Geethan, A., Jayaseelan, V., & Francis Xavier, J. (2020). Experimental investigation on diffusion bonding of dissimilar metals. *AIP Conference Proceedings*, *2283*(October). https://doi.org/10.1063/5.0025159

Su, Y., Jiang, F., Xiao, Z., Long, M., Wu, F., Wu, M., & Ye, P. (2022). Influence of sintering pressure on microstructure and tribological properties of Copper–Tin composites containing graphite and MoS2. *Surface Topography: Metrology and Properties*, *10*(4), 45019.

Vairamuthu, J., Stalin, B., Sivakumar, G. D., Fazil, B. M., Balaji, R., & Natarajan, V. A. (2021). The effect of process parameters for synthesized copper metal matrix using stir casting process. *Materials Today: Proceedings*, *45*(xxxx), 1970–1974. https://doi.org/10.1016/j.matpr.2020.09.262

Vaisakh, S. S., Mahesh, K. V., Balanand, S., Metz, R., Hassanzadeh, M., & Ananthakumar, S. (2015). MAX phase ternary carbide derived 2-D ceramic nanostructures [CDCN] as chemically interactive functional fillers for damage tolerant epoxy polymer nanocomposites. *RSC Advances*, *5*(21), 16521–16531. https://doi.org/10.1039/c4ra16518g

Vinoth, R., Patil, I. M., Pandikumar, A., Kakade, B. A., Huang, N. M., Dionysios, D. D., & Neppolian, B. (2016). Synergistically Enhanced Electrocatalytic Performance of an N-Doped Graphene Quantum Dot-Decorated 3D MoS2-Graphene Nanohybrid for Oxygen Reduction Reaction. *ACS Omega*, *1*(5), 971–980. https://doi.org/10.1021/acsomega.6b00275

Wang, B., Zhang, Q., Wang, M., Zheng, Y., & Kong, X. (2020). A predictive model of milling surface roughness. *The International Journal of Advanced Manufacturing Technology*, *108*, 2755–2762.

Wang, L., Tong, Y. G., Zhou, C., Li, Y. J., Liu, J., Cai, Z. H., Wang, H. D., & Hu, Y. L. (2023). Self-lubricating Ti3SiC2 strengthening Cu composites with electrical conductivity and wear resistance trade off. *Tribology International*, *187*, 108724.

Yang, Z., Xu, J., Qian, Y., Liu, H., Zuo, J., Ma, K., & Li, M. (2023). Electrical conductivities and mechanical properties of Ti3SiC2 reinforced Cu-based composites prepared by cold spray. *Journal of Alloys and Compounds*, *946*, 169473.

Yehia, H. M., Ali, A. I., & Abd-Elhameed, E. (2023). Effect of exfoliated MoS2 on the microstructure, hardness, and tribological properties of copper matrix nanocomposite fabricated via the hot pressing method. *Transactions of the Indian Institute of Metals*, *76*(1), 195–204.

APPENDIX

APPENDIX-A

A-1. Mass of sample before and after wear

Samples used for wear test	Before (g)	After (g)	mass loss (g)
S1	2.229	2.2195	0.0095
S2	2.7811	2.7708	0.0103
S3	2.8782	2.8697	0.0085
S4	2.752	2.7464	0.0056
S5	2.3054	2.302	0.0034

A-2. Input and output responses of multi response gray relation analysis

	Input Parameters				Output value(Response)				
Run	Cu wt%	Ti3SiC2	MoS2	GO	Porosity % (Minima)	Hardness HV (Max)	Wear rate mmpy (Minima)	Compression Mpa (Max)	COF (Minima)
S1	98	1	1	0	3.55	241.67	0.25	397	0.25
S2	98	1	0	1	1.83	309.87	0.23	365	0.45
S3	97	1	1	1	2.83	319	0.21	473	0.225
S4	96	2	1	1	2.26	346.97	0.14	524	0.22
S5	95	3	1	1	2.11	379.13	0.09	540	0.165

APPENDIX-B

B-1. Micro-Hardness Results of some samples (Form Vickers Hardness)

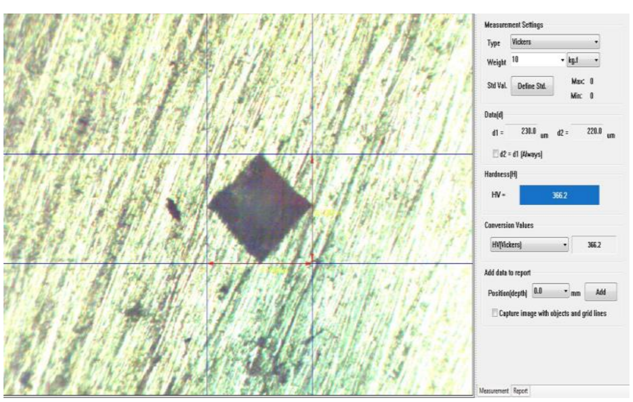

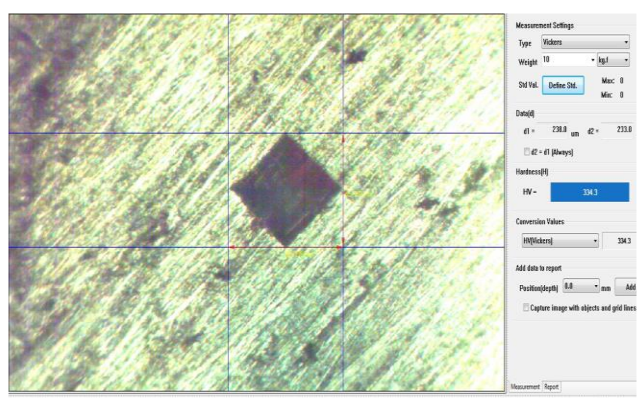

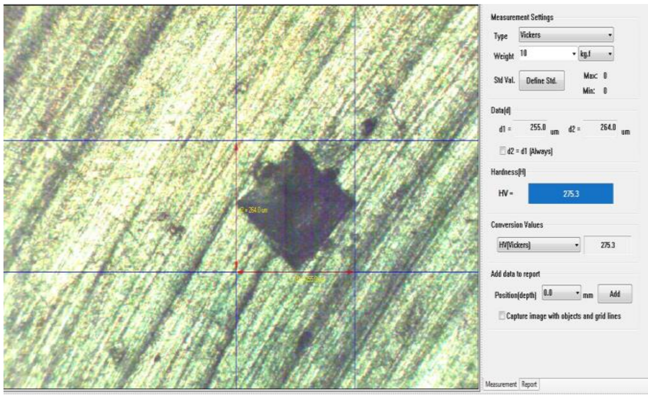

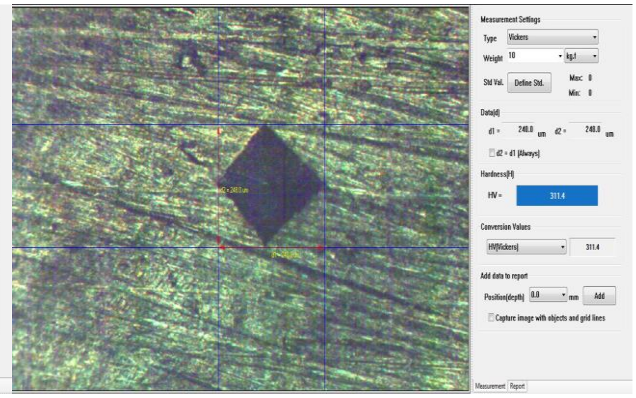

APPENDIX-C

C-1. Fabricated sample 3 and mold used to fabricate